

**Dust Distribution in Gas Disks.
A Model for the Ring Around HR 4796A**

H.Hubertus Klahr

and

D.N.C. Lin

UCO/Lick Observatory, University of California, Santa Cruz, CA 95064

ABSTRACT

There have been several model analyses of the near and mid IR flux from the circumstellar ring around HR4796A. In one set of models, the 10 and 18 μm IR flux has been attributed to the reprocessing of stellar radiation by μm -size particles. Since these particles are being blown away, on a dynamical time-scale, by the radiation pressure of HR4796A, they must be continually replenished by the collisional fragments of larger particles. If the ring appearance persisted for the life span (8×10^6 yr) of HR4796A, a parent-particle reservoir with a total mass greater than $300M_{\oplus}$ would be needed. In order to avoid being conspicuous at longer wavelengths, most of the mass must be contained in parent particles larger than 20 – 40 cm. In other models, it has been suggested that the IR flux from the rings is emitted by sufficiently large particles that survive the radiative blow out by their host star. In a gas free ring, greater than 3.2 μm -size particles would survive radiative blow out and a total of $10^{-2}M_{\oplus}$ would be adequate to account for the observed IR flux. But, in the vicinity of a young star, the possibility that the dust ring is embedded within a residual protostellar gas disk cannot be ruled out. In a gas-rich environment, larger sizes ($> 100\mu m$) are needed for the particles to survive the radiative blow out. The total dust mass required to account for the IR flux is $< 10^{-1}M_{\oplus}$. The combined influence of gas and stellar radiation may also account for the observed sharp inner boundary and rapidly fading outer boundary of the ring. The pressure gradient induced by a small (10%) amplitude variation in the surface density distribution of a low-mass gaseous disk would be sufficient to modify the rotation speed of the gas. The resulting hydrodynamic drag on modest-size ($> 100\mu m$) particles would be adequate to compensate for the turbulent stirring, radiative drag and radiation pressure such that they remain gravitationally bound to the system. The required surface density variation of the gas may be induced by 1) the perturbation of a low-mass planet or the binary companion HR 4796B, 2) the photo evaporation of the disk, or 3) from the variations in the viscous angular momentum transport and mass diffusion rate in the disk. We show that the structure of the dust ring is preserved during and after the gas is being depleted such that similar rings may be common among early-type stars.

Subject headings: circumstellar matter, planetary systems, stars: formation

1. Introduction

The observational discoveries (Smith & Terile 1984) of β Pic type dusty rings provide tantalizing hints of residual planetesimal disks similar to the Kuiper belt may exist around other stars (Artymowicz 1997). Perhaps the most intriguing dust rings are those around HR 4796A (Schneider *et al.* 1999) and HD 141569 (Weinberger *et al.* 1999). The sharp surface density variations near the ring boundaries of HR 4796A are remarkably similar to that found around Saturn’s F ring (Cuzzi *et al.* 1984) and Uranus’ ϵ ring (Elliot & Nicholson 1984). Under the action of viscous stress, these differentially rotating disks have a general tendency to diffuse in the radial direction (Lynden-Bell & Pringle 1974). The expansion of planetary rings are prevented by the tidal torques of nearby shepherding satellites (Goldreich & Tremaine 1979, 1982). The structural resemblance between circumstellar and planetary rings naturally leads to the conjecture that the former, too, may be perturbed by nearby hypothetical planets (Jura *et al.* 1995). The reported azimuthal brightness asymmetry (Telesco *et al.* 2000) provides a supporting evidence for the scenario that the ring may be gravitationally perturbed by a planetary or stellar companion (Wyatt *et al.* 2000).

Another motivation for invoking the embedded planet scenario is the perseverance of the ring itself. The NICMOS image shows that the surface brightness has a maximum at 70 AU with a sharp decline at the smaller radii and an inner cutoff near 50 AU. Outside this region, the surface brightness decreases more gradually with radius to less than half of the peak brightness at 90AU (Schneider *et al.* 1999). The observed ratio of flux from the ring to that from the star increases with wavelength at 1.1 and 2.6 μm , indicating the mean particle size is larger than these wavelength. But, using the flux ratio at 10 and 18 μm and assuming a Mie emissivity, Telesco *et al.* (2000) inferred a “characteristic” diameter for the dust particles to $\sim 2 - 3\mu m$ which is in contrast to the lower particle-size limit of $10\mu m$ inferred from the $60\mu m$ radiation by Jura (*et al.* 1993). The observed spectral energy distribution (SED) with wavelength $\lambda = 10 - 10^3\mu m$ (Koerner *et al.* 1998) has been modeled. Using single-size particles ($> 100\mu m$), Augereau *et al.* (1999) were able to fit the observed SED between $10 - 10^2\mu m$ but not the resolved images of the ring. Both the SED and the resolved images were better modeled with reprocessing by particles with a power-law collisional particle-size distribution (Heller 1970, Mathis *et al.* 1977) with adopted minimum (a_{\min}) and maximum (a_{\max}) sizes of $\sim 10\mu m$ and a few meters respectively. In these models, since the models are applied to SED in the wavelength range of $10 - 10^3\mu m$, the actual values chosen for a_{\min} and a_{\max} do not significantly affect the actual match.

With the stellar luminosity $L_{\star} = 35L_{\odot}$, small particles, if they exist, would be blown away by the radiation pressure on the time-scale of a few hundred years (Backman & Paresce 1993). In the models adopted by Augereau *et al.* (1999), all particles with sizes larger than a_{\min} would survive the radiative blow-out effect. But for the models proposed by Telesco *et al.* (2000), the

“characteristic-size” particles would not be able to remain. In a companion paper, Wyatt *et al.* (2000) suggested that these small particles are probably the collisional fragment of a population of larger particles. In this replenishment scenario, it is still essential for the parent particles to have an adequate reservoir of total mass to replenish the μm -size particles for HR 4796A’s life span $\tau_\star = 8 \times 10^6$ yr (Stauffer *et al.* 1995, Jayawardhana *et al.* 1998). In order to be consistent with the observed SED and ring structure, most of these parent particles must also be located within 70 ± 20 AU and have a surface density comparable to or less than that inferred by Augereau *et al.* (1999). One or more nearby planets may provide both the supply and confinement mechanism for the parent particles.

An important issue to be resolved is the required mass for such perturbers. In HR 4796A, such confining planets must either form or migrate to the vicinity of the rings (which is well beyond the orbit of Neptune) within τ_\star . In conventional theories, the first stage of planetary formation is the emergence of planetesimals and solid cores (Safronov 1969; Wetherill 1980). Only after these cores have acquired a few Earth-masses does dynamical accretion of gas become possible (Pollack *et al.* 1996). But, beyond the orbit of Neptune, the formation of a few Earth masses core requires at least several 10^7 yr ($> \tau_\star$) unless the mass of solid material is much larger than that inferred from the minimum mass solar nebula model (Lissauer 1993). Assuming an initial surface density 10-20 times that of the minimum mass solar nebula (which corresponds to 150-300 M_\oplus within the annulus between $\sim 58 - 82$ AU), Kenyon *et al.* (1999) found it possible to form planetesimals larger than 10^3 km within 10^7 yr. They further suggested that gravitational perturbation by these large objects may excite large velocity dispersion that may lead to disruptive collisions. However, if this assumed surface density of the dust particles is augmented for the solar composition, the inferred mass of the gaseous ring ($\sim 0.05 - 0.1 M_\odot$ within 70 ± 12 AU) would make it gravitationally unstable. Cameron (1978) and Boss (1998) have suggested that gravitational instability in the disk may indeed lead to the formation of giant planets directly from the disk gas. But, some numerical simulations show that the growth of non axisymmetric perturbations excited by gravitational instability are more likely to induce efficient transfer of angular momentum in the disk rather than fragmentation (Nelson *et al.* 1998, Burkert & Bodenheimer 1996). The initial surface density required for this conjecture is also large compared with the mass inferred for the outer regions of typical protostellar disks (Beckwith & Sargent 1993a).

In this paper, we examine the persistence of the dust ring structure around HR 4796A. Since the host star is only 8×10^6 yrs old, we hypothesize the existence of some residual gas analogous to those found around several young stellar objects with similar ages (Beckwith *et al.* 1990, Beckwith & Sargent 1993b, Zuckerman *et al.* 1995, Hartmann *et al.* 1998). An upper limit 1-7 M_\oplus of gas has been inferred from the mm continuum radiation by Greaves *et al.* (2000). (A larger gas mass may exist if a substantial amount of heavy element is depleted from the gas phase and is stored in particles larger than a few mm.) We explore the interaction between the dust, radiation, and residual gas in the disk. In §2, we briefly recapitulate the physical interaction between particles, stellar radiation, and residual gas. We show that the hydrodynamic drag tends to promote the

effect of radiation pressure and increase the critical particle size for radiative blow out. In §3, we provide some constraints on the size and total mass of particles in the ring around HR 4796A. We show that variations in the surface distribution of the gas provide a favorable condition for modest (more than 100 μm) size particles to congregate into a dust ring. This ring structure is preserved during and after the depletion of the disk gas. We suggest that these particles provide a supply of the dominant contributors to the IR emission of the dust ring. Finally in §4, we discuss the implications of these results on planet formation and the ubiquity of similar rings around other early type stars.

2. The Dynamics of Residual Dust Particles

In this section, we examine the interaction between stellar radiation, residual disk gas, and dust particles of various sizes.

2.1. The gaseous disk

For illustrative purpose, we consider a simple model in which a disk of dust particles is embedded in a residual gaseous disk. The only free parameters in this model are those which describe the gas surface density $\Sigma(R)$ as a function of the disk radius R . All other gas properties are deduced in a self-consistent way.

The qualitative results presented here depend on the gross global gas distribution in the disk and are insensitive to the detailed expression of $\Sigma(R)$. In principle, the Σ distribution is determined by the efficiency of angular momentum transfer (e.g. via viscosity from turbulence) in the disk and the tidal perturbation by planetary or stellar companions. The former mechanism generally leads Σ to attain a power law function of R in most regions of the disk (Lin & Bodenheimer 1981; Ruden & Lin 1986). The latter process leads to a localized Σ variation such as gaps (Lin & Papaloizou 1979; 1993) and confined rings (Goldreich & Tremaine 1978). Although low-mass companions may not be able to induce the formation of a gap, they can nevertheless introduce variations in the surface density of the disk. Self-gravitational effects will not affect the disk structure as the surface density in our models is always orders of magnitude smaller than any critical value (see Toomre 1964). For computational purpose (e.g. to produce our plots), we adopt the following generic prescription in which the global variation of Σ is non monotonic:

$$\Sigma = \Sigma_0 \times \begin{pmatrix} d \left(\frac{R}{R_0} \right)^{-2.5} & \text{if : } R < R_1 \\ e^{-\frac{(R-R_0)^2}{\delta R_0^2}} & \text{if : } R_1 \leq R \leq R_0 \\ \left(\frac{R}{R_0} \right)^{-2.5} & \text{if : } R > R_0 \end{pmatrix} \quad (1)$$

where d is a model parameter which determines the amplitude of a local maximum. The magnitude

of Σ at some fiducial radial location R_0 is set to be Σ_0 . For $R < R_1$ and $R > R_0$, Σ decreases monotonically with R following a power law (with an index -2.5) which is somewhat steeper than that for the minimum mass solar nebula model (Hayashi *et al.* 1985). But in the outer region of the disk, Σ is likely to decline more rapidly with R as inferred from observation (Mundy *et al.* 1996, Hartmann *et al.* 1998). Since our results are insensitive to the detailed nature of the global radial dependence of Σ , we choose such a power law so that the disk mass remains finite at large R .

The inner and outer regions of the disk are connected through a transition zone at $R_1 \leq R \leq R_0$. In this zone the surface density has the shape of a Gaussian with a width of δR_0 . The value of R_1 is set to satisfy $(R_1 - R_0) = \delta R_0(2.5\ln(R_1/R_0) - \ln d)^{1/2}$ such that Σ is continuous. In all our models, we choose $d < 1$ which is reasonable because the continuum flux in the mid-IR wavelength range is observed to be more intense than that in the near-IR range in several protostellar disks (Hillenbrand *et al.* 1998). One possible interpretation is that these disks are more depleted in the inner region or better preserved in the outer region as in the context of circumbinary disks (Jensen & Mathieu 1997). On the theoretical side, such a Σ variation is expected if a) the viscosity decreases rapidly with radius (Ruden & Pollack 1991), b) the inner region is depleted by either a stellar or a disk wind (Shu *et al.* 1994, Konigl & Ruden 1993), c) HR4796A is a A0V star and a strong source of UV radiation which could lead to photo evaporation in some regions of the disk (Shu *et al.* 1993) and quench gas infall along the rotation axis and onto the inner regions of the disk (Yorke *et al.* 1995), d) the disk is depleted by the formation of one or more planets which are expected to first emerge in the inner regions of the disk (Jura *et al.* 1993), or e) the structure of disk around HR4796A may be tidally perturbed by the stellar companion HR4796B (Augereau *et al.* 1999), especially if the binary orbit is eccentric (Korycansky & Papaloizou 1995). The difference between the inner and outer regions of the disk can be minimized by setting d close to unity. Finally, the Σ variation in the transition region $R_1 \leq R \leq R_0$ can also represent a tidal perturbation of a nearby embedded planetary companion.

The value of Σ_0 is set such that the mass $M_g = 2\pi \int_{R_0-\delta R_0}^{R_0+\delta R_0} R\Sigma(R)dR$ contained within a ring centered on R_0 with a half width δR_0 is to be specified as a model parameter. This mass is to be spread over a ring with a half width $\delta R_0 = 10 - 20$ AU centered on a radial location $R_0 = 70$ AU. In our models M_g is 1-100 Earth masses (M_\oplus). The corresponding Σ is orders of magnitude smaller than that for the minimum mass solar nebula model at a similar distance from the central star (Hayashi, Nakazawa & Nakagawa 1985).

The outer regions of the disk are optically thin such that every dust particle in the disk receives direct irradiation from the central object. The particles are heated to the local black body temperature (small grains may be hotter because they cannot radiate efficiently, Chiang & Goldreich 1997). The luminosity and mass of HR 4796A are $L_\star = 35L_\odot$ and $M_\star = 2.5M_\odot$ respectively (Jura *et al.* 1993). The temperature of the dust grains can be given by:

$$T_d = \left(\frac{L_\star}{16\pi a R^2} \right)^{1/4} \quad (2)$$

where a is the radiation density constant. This upper limit estimation holds for particles larger than the typical wave length of the radiation and assuming an albedo of zero. A more careful treatment of the optical properties of the particles is not necessary in the context of the effects studied in this paper.

If gas molecules collide frequently with the dust particles, they can also attain a similar temperature, $T_{high} = T_d$. In the low gas density limit, however, thermal conduction between the dust and the gas is less efficient than the gas radiative processes. As a consequence of this thermal imbalance, the gas temperature may decrease to a minimum value ($T_{low} = 10\text{K}$) which is comparable to that of the radiation background field (Preibisch, Sonnhalter and Yorke 1995; Yorke & Lin in preparation). In general, $T_{low} < T_{gas} < T_{high}$ and the associated sound speed $c_s = \sqrt{T_{gas} * R_{gas} / \mu}$, where R_{gas} is the gas constant and μ the mean molecular weight (i.e. $\mu = 2.353$ for an $He - H_2$ mixture). The disk thickness is determined by its pressure scale height $H_p = c_s / \Omega$ where $\Omega \equiv (GM_*/R^3)^{1/2}$ is the Keplerian frequency. At $R = 70$ AU, $0.03 < H_p/R < 0.1$ for the low and high temperature limits. For the parameters we have adopted, the disk gas is likely to be in the low temperature and small thickness range. The local gas density in the midplane of the disk can be estimated as $\rho = \Sigma/2H_p$ and the pressure p becomes $p = c_s^2 \rho$.

The azimuthal orbital frequency of the gas (ω) is given by the condition for hydrostatic equilibrium between the gravitational potential of the central object and the sum of centrifugal acceleration and the radial pressure gradient

$$\frac{GM_*}{R^2} = \omega^2 R - \frac{1}{\rho} \nabla p, \quad (3)$$

which leads, in first order approximation, to a local deviation dV from the Keplerian profile of (see Whipple 1972)

$$dV \equiv (\omega - \Omega)R = V_\phi - \Omega R = \frac{1}{2\Omega\rho} \nabla p \simeq \frac{c_s^2}{2\Omega R} \frac{\partial \ln \rho}{\partial \ln R} \quad (4)$$

where $V_\phi = \omega R$ is the azimuthal speed. In §2.4, we consider the case that this angular frequency may be modified by the particles' drag when they become the dominant constituent of the disk.

Results under specific assumptions for the free parameters of this model will be discussed in the §3.

2.2. Radial drift of dust grains

The particles are drifting radially under two independent physical effects: 1) hydrodynamic drag by the gas and 2) the radiation pressure of photons emitted by the central object.

2.2.1. Departure from Keplerian flow

While the pressure gradient induces the gas to attain a finite dV , the particles' motion is determined by the gravity of the central star, the hydrodynamic drag by the disk gas, and the drag and pressure by the stellar radiation. Radial inward and outward drift of the particles can be generated by the non-Keplerian motion of the gas. Small particles are well coupled to the gas, thus they also move on non-Keplerian orbits provided their Stokes number $St \equiv \tau_f \Omega \ll 1.0$ (Weidenschilling 1977). The friction time for a spherical particle in the Epstein regime (e.g. Klahr & Henning 1997) is given by

$$\tau_f = \frac{a_d \rho_d}{c_s \rho} = \frac{3m_d}{4A_d c_s \rho}, \quad (5)$$

where a_d is the particle's radius, m_d its mass, $A_d = \pi a_d^2$ its cross section, ρ_d its density, c_s the thermal velocity of the gas and ρ the local gas density. In the case of transonic velocities (which is irrelevant in our model) c_s has to be replaced by $\sqrt{c_s^2 + dv^2}$ with the relative velocity (dv) between the particle and the gas (H. Yorke 1999, private communication). The critical particle size which demarcates the small and large particle size range then becomes

$$a_0 = \Sigma / 2\rho_d \quad (6)$$

which is a few cm for a minimum mass solar nebula model at 70 AU and smaller for a depleted gaseous disk. In our standard models (see Sect. 3.5.1 and Sect. 3.5.2), $a_0 = 0.06$ cm at R_0 .

In the solar system today, the absence of gas makes $St \gg 1$ for all particles. Modest-size particles spiral inwards due to the Poynting Robertson effect (see below), but spherical particles (with $\rho_d = 2.5 \text{ gm cm}^{-3}$) with size

$$a_d < a_1 \equiv \frac{3}{16\pi} \frac{L_\star}{GM_\star c \rho_d} \sim 3.2 \mu\text{m} \quad (7)$$

would be blown out by the radiation pressure on hyperbolic orbits as “beta meteorites” (see Grün *et al.* 1985) on a time-scale comparable to the local dynamical time-scale $\tau_d \sim \Omega^{-1} \sim 10^2$ yr (see below). For our considerations we neglect particles smaller than the typical wavelength of the radiation (No Mie scattering).

Larger particles would remain bound to the host star. They can even remain on a circular orbit with a sub Keplerian azimuthal velocity

$$v_\phi^* = \sqrt{\frac{GM_\star - \frac{L_\star A_d}{4\pi m_d c}}{R}}, \quad (8)$$

where v_ϕ^* denotes the particles theoretical velocity in the absence of gas, which is an important quantity (see below). While the particles are orbiting around the central star they also experience a radiative head wind due to the aberration of its photons. In gas-free environments, such as our own solar system, this Poynting-Robertson radiative drag effect induces the azimuthal velocity

(v_ϕ) of small particles to change at a rate

$$\dot{v}_\phi = -\frac{L_\star}{4\pi R^2} \frac{A_d}{m_d c^2} v_\phi. \quad (9)$$

This process leads an inward drift for all remaining particles with $a_d > a_1$.

In a gaseous environment, the combined influence of hydrodynamic and radiative drag induces the particles' azimuthal velocity to change at a rate

$$\dot{v}_\phi = -\frac{(v_\phi - V_\phi)}{\tau_f} - \frac{L_\star}{4\pi R^2} \frac{A_d}{m_d c^2} v_\phi. \quad (10)$$

If τ_f is small in comparison to the relevant evolutionary time-scales (see Fig. 1 and Fig. 2), an equilibrium would be rapidly established with $\dot{v}_\phi = 0$ so that

$$v_\phi = \frac{V_\phi}{1 + \tau_f \left(\frac{L_\star}{4\pi R^2} \frac{A_d}{m_d c^2} \right)}. \quad (11)$$

Substituting τ_f , we find

$$v_\phi = \frac{V_\phi}{1 + \left(\frac{L_\star}{4\pi R^2} \frac{3}{4c^2 c_s \rho} \right)} \quad (12)$$

which is independent of particle sizes (as long as $St \ll 1$ and the particles are larger than the wavelength of the radiation)!

Around young stellar objects where the particles are embedded in a gaseous circumstellar disk environment, the term $dv \equiv v_\phi - V_\phi$ (see Fig. 1) is typically less than of 1 mm/s at 70 AU while $dV \sim 10^3$ cm/s. Note that the Poynting Robertson effect is insignificant until Σ is depleted below $3L_\star/8\pi R^2 c^2 \Omega$ which is not only more than four orders of magnitude below that for our standard model and that inferred from mm continuum radiation for typical protostellar disks but also smaller than that inferred for the CO gas around some young stellar objects (Zuckerman *et al.* 1995). (The actual gas content may be even larger if a significant amount of CO gas is depleted due to grain condensation.) Thus, in our estimate of the particles' motion, we only consider contributions from dV and neglect the Poynting Robertson effect.

2.2.2. Radial drift

In addition to the radiative drag in the azimuthal direction, the stellar photons also exert on the particles a radiative pressure in the radial direction. In general, the radial drift v_r of small particles (with $St < 1$) results from the non-Keplerian motion and the radial radiation pressure can be obtained from the radial component of the equation of motion such that

$$\frac{\partial v_r}{\partial t} = -\frac{v_r}{\tau_f} + \frac{v_\phi^2}{R} - \frac{GM_\star}{R^2} + \frac{L_\star}{4\pi R^2} \frac{A_d}{m_d c}. \quad (13)$$

In order to simplify work we define $\Omega^*(\equiv v_\phi^*/R)$ which is the orbital frequency with respect to the radial radiation pressure (see Eq. 8). Note that $\Omega^* < \Omega$ in general. Thus it follows

$$\frac{\partial v_r}{\partial t} = -\frac{v_r}{\tau_f} + \frac{(\Omega^*R + dV^*)^2}{R} - \Omega^{*2}R. \quad (14)$$

Here $dV^* \equiv v_\phi - \Omega^*R$ denotes the deviation of the gas from the modified Keplerian orbit. Since the radius dependence of gravity and radiation pressure is identical, the outward radiation pressure effectively reduces the gravitational attraction on the particles imposed by the host star everywhere (Gustafson 1994).

The “characteristic size” of particles inferred by Telesco *et al.* (2000) is smaller than a_1 such that they are expected to be blown away by the radiation pressure of HR4796A. In order to remove this dilemma, Wyatt *et al.* (1999) suggested that although these small particles are continually being blown out, they are also being replenished by collisional fragmentation of larger particles which are not significantly affected by the radiation pressure. In a gas free environment, the parent body size must be larger than a_1 .

But, around many young stellar objects, small particles are embedded in a residual gaseous background. The gas generally does not directly experience the radiation pressure because its molecular opacity is too small. Thus, the gas azimuthal speed (V_ϕ) is independent of L_\star and it is given by eq. (3). The discussions in §2.2.1 indicate that particles with $St < 1$ (or equivalently with $a_d < a_0$) have $v_\phi \sim V_\phi$ (see eq. 12). As the hydrodynamic drag forces these small particles to nearly corotate with the gas, they attain a finite v_r as a consequence of being out of hydrostatic equilibrium. When a steady state is established,

$$v_r = \tau_f 2\Omega^* dV^* \quad \text{for } St \ll 1, \quad (15)$$

in the limit that the quadratic term dv^2 is small in comparison to Ω^*Rdv^* (cf Weidenschilling 1977; He used another definition of dV^*). The sign of dV^* can now be negative or positive, depending on whether the particle is less or even more sub-Keplerian than the gas. Relatively large particles follow in a similar fashion,

$$v_r = dV^* \quad \text{for } St = 1, \quad (16)$$

and

$$v_r = \frac{2dV^*}{\Omega^*\tau_f} \quad \text{for } St \gg 1. \quad (17)$$

Note that the effect of radiation pressure decreases with the particle size. From this equation one can deduce that in regions where $dV > 0$ (as a positive or a negative gas pressure gradient), all the particles would migrate outwards since their azimuthal speed is always slightly hyper-Keplerian, just like the gas. But in the more common situation where $dV \leq 0$ (which corresponds to a negative gas pressure gradient as expected in unperturbed regions of protostellar disks), hydrodynamic drag is more important than radiative drag for all particles with

$$a_d > a_2 \equiv -\frac{3L_\star}{32\pi R^2 c \Omega \rho_d dV} \quad (18)$$

so that they undergo orbital decay. In contrast, particles with $a_d < a_2$ are blown away by the stellar radiation pressure (see Fig. 1 and Fig. 2). This minimal size for the given parameters of HR 4796A is $a_2 \sim 100 - 200 \mu\text{m}$ for almost all disk radii R . Only at those location where variations in Σ lead to a reduction in dV is a_2 greater than $500 \mu\text{m}$. In the location where dV vanishes or attains a negative value, a_2 becomes infinite and particles of all sizes (including planets) are prevented from inward radial drift.

We note that the magnitude of a_2 is larger than a_1 in eq(7) by a factor $\sim (R^2/H_p^2)(d\ln\rho/d\ln R)^{-1} \sim 10 - 100$ because the small particles are forced to corotate with the gas such that a centrifugal balance is always maintained. Thus, if they are embedded in a residual gaseous disk, the “characteristic-size” (μm -size) particles in HR 4796A inferred by Telesco *et al.* (2000) must be supplied by parent bodies which are at least two order of magnitude larger than them.

In a gaseous disk environment, all particles with a_d smaller than both a_0 and a_2 are blown away by the radiation pressure on the dynamical time-scale τ_d . In the limit that $a_0 > a_2$, particles with sizes $a_0 > a_d > a_2$ can achieve both positive and negative radial drift velocities depending on the local gas pressure gradient. In §3, we present numerical results to show that these changes in the direction of particles’ radial drift lead to the particles’ accumulation into rings. Note that the value of a_2 does not directly depend on Σ . As the disk gas is depleted, neither dV nor a_2 are strongly affected. But, a_0 is linearly proportional to Σ . When a_0 decreases below a_d of some particles, they decouple from the gas and their azimuthal velocity becomes closer to the local modified Keplerian value v_ϕ^* (see eq. 8). Since their a_d is larger than a_2 initially and a_2 decreases, the radiation pressure and the Poynting Robertson effect have a weaker effect than the hydrodynamic drag throughout the evolution such that their radial drift velocity is described by eq. 17. Eventually, the depletion of the residual gas increases τ_f and reduces v_r .

2.3. Constrains on the disk profile

We already noted that the trapping mechanism for particles is located at places, where the disk becomes Keplerian, as the radial pressure gradient vanishes, *i.e.*

$$\nabla p = \nabla (c_s^2 \rho) = \nabla (c_s \Sigma \Omega) = 0. \quad (19)$$

Since $\Omega \sim R^{-3/2}$, the general criterion for the ring formation is

$$c_s \Sigma \propto R^{3/2}. \quad (20)$$

This criterion can now be used to determine the local shape of the Surface density profile. We consider three distinct cases: 1) an isothermal disk ($T = T_{low}$), 2) an optically thin disk in radiation equilibrium ($T = T_{high}$), and 3) an optically thick viscous disk.

In the isothermal case c_s is constant such that the trapping mechanism requires Σ to increase locally as $R^{3/2}$ regardless its magnitude and radial extent. In the standard optical thin case,

(perhaps most relevant to the case of HR4796A), $c_s \sim R^{-\frac{1}{4}}$ as $T \sim R^{-\frac{1}{2}}$. The necessary power-law R -dependence in Σ is only slightly steeper than in the previous case: *i.e.* $\Sigma \sim R^{\frac{7}{4}}$.

In an optically thick disk which is heated by the local viscous dissipation, the disk's mid plane temperature $T_c = T_e (3\tau_r/8)^{1/4}$ where the vertical optical thickness $\tau_r \approx \kappa\Sigma/2$ and the Rosseland mean opacity $\kappa = \kappa_o T_c^2$ (Lin & Papaloizou 1985). If the disk is approximately in a steady state, its effective temperature $T_e \propto R^{-\frac{3}{4}}$ (e.g. Lynden-Bell & Pringle 1974, Bell *et al.* 1997) such that $T_c \propto \kappa_o^{1/2} T_e^2 \Sigma^{1/2} \propto R^{-3/2} \Sigma^{1/2}$. Particles are trapped in regions where $\Sigma \propto \kappa_o^{-1/5} R^{9/5}$ which is similar to the isothermal and the optically thin cases.

The dominant contributors to the disk opacity are grains. Across some critical locations (dust destruction zone) in the disk where the grains sublimate, the opacity increases mainly through changes in the scaling constant κ_o (Ruden & Lin 1986). Particles may be trapped in regions where $\kappa_o \propto R^9$. A full 2-D detailed model is needed to address the issue whether such a transition may indeed be a viable effect to prevent dust in form of meter sized solid bodies from drifting into the sun and help collect bodies at certain transition radii from the sun to form the terrestrial planets. For the present context, the ring around HR 4796 A is well outside the ice and silicate destruction zones.

2.4. Particle-dominant flow

In the above discussion, we neglect the feedback effect of hydrodynamic drag on the gas flow. In principle, the gas flow may be perturbed by the motion of the particles when the particles dominate in mass surface density (Σ_d) over the surrounding gas (Nakagawa, Sekiya, & Hayashi 1986). In the Kuiper Belt today, no sign of residual gas has been detected. Gas may be preferentially depleted prior to the depletion of the dust particles. When the surface density of the gas (Σ) decreases below that of the dust (Σ_d), the hydrodynamic drag between them may induce the gas to comove with the particles rather than forcing the particles to corotate with the gas. In reality, however, the only particles which can provide an efficient momentum transfer with the gas are those with sizes $a_d \ll a_0$ (Nakagawa *et al.* 1986). During the depletion of gas, a_0 decreases with Σ , leading to a reduction in the total fraction of particles which are well coupled with the gas. Thus, the gas speed is unlikely to be significantly affected by the particles' drag effect.

For those regions of the disk with $\Sigma > \Sigma_d$, gas flow would be affected by the hydrodynamic drag of the particles near the midplane of the disk if the total mass density of the particle $n_d m_d$ exceeds the gas density $\rho \sim \Sigma/H_p$ (Weidenschilling & Cuzzi 1993). (Similarly, particle accumulation due to variations in the radial drift speed may also lead to local enhancement of particle density.) The average mass density of the particles ρ_{dust} is determined by their scale height $H_d = \sigma_d/\Omega$ where σ_d is the velocity dispersion of the particles. In a turbulent medium, the particles are being stirred by the dispersive motion of the gas. Since the turbulent speed of the gas is unlikely to exceed its sound speed, particles with $a_d > a_0$ would sediment toward the mid plane

and attain a scale height $H_d < H$. With a substantially sub sonic turbulent speed, sedimentation is also possible for sufficiently small ($a_d < a_0$) particles which couple well with the gas. Only after ρ_{dust} of the small ($a_d < a_0$) particles has exceeded the gas density $\sim \Sigma/2H$, would the gas motion be forced to corotate with the small particles' Ω^* of the rather than ω . Without a significant differential motion between them and the gas, particles with $a_1 < a_d < a_0$ would not undergo any further orbital migration. But larger ($a_d > a_0$) particles are less affected by the radiation pressure and have a larger v_ϕ^* . Gas drag induced by the residual headwind would continue to drive the larger particles inward though at a much reduced pace.

But, the optical depth of HR4796 A is well below unity and

$$\rho_{dust} = \frac{2L_{disk}}{3\pi L_*} \frac{\rho_d a_d}{H_d} \quad (21)$$

(see eq. 26 below). For particles of $a_d = 200\mu\text{m}$ the density is $\rho_{dust} \ll 6.3 \times 10^{-17} \text{g cm}^{-3}$, which is well below the gas density inferred from the minimum mass solar nebula model. For those models we have adopted in this paper, particles have negligible drag effect on the motion of the gas.

3. Models for HR 4796A

In this section, we present a scenario for the ring structure around HR 4796A. First, we revisit the two existing models for particle size distribution by analyzing the preferred size of particles for retention. We describe a simple quasi static model in which we assume that HR 4796A had initially a circumstellar gas and dust disk around it. We then show that a dust disk will evolve into a ring structure with sharp edges. We argue such a structure would be preserved after the gas is depleted.

3.1. Replenishment of a population of μm -size particles

First, we examine the implication of the scenario proposed by Telesco *et al.* (2000) in which the dominant contributors to the 10 and 18 μm radiation from the ring around HR 4796A are μm -size particles. Since the “characteristic” size of the particle is comparable to the wavelength of the photon, the reprocessed radiation by the disk particles

$$L_{disk} = QL_* \frac{A_d}{4\pi R^2} \frac{M_{char}}{m_d} \quad (22)$$

where Q is the albedo and assumed to be one for large particles and dR the radial width of the dust ring. Assuming *SiO*-dust particles which have spherical shape and a density $\rho_d = 2.5 \text{gm cm}^{-3}$, the total mass of those particles with “characteristic” sizes is

$$M_{char} = \frac{16\pi}{3} \frac{L_{disk}}{L_*} R^2 \rho_d a_d. \quad (23)$$

The total IR luminosity of the ring is estimated to be $L_{disk}/L_{\star} = 5 \times 10^{-3}$ (Jura *et al.* 1993) so that

$$M_{char} \approx (a_d/1\text{cm}) \times 2.3 \times 10^{29} g \approx (a_d/1\text{cm}) \times 38M_{\oplus}. \quad (24)$$

For the all particle size to be at the “characteristic” size $a_c = 1 - 2\mu m$, one would need $M_{char} \sim 4 - 8 \times 10^{-3} M_{\oplus}$.

If the IR emitting particles are smaller than both a_1 and a_2 they would be blown away from the ring region on a dynamical time-scale $\tau_d = \Omega^{-1} \sim 10^2$ yr in both gas-rich and gas-free environment. Over the life span of HR4796A ($\tau_{\star} = 8 \times 10^6$ yr), an amount $M_{lost}^{char} \approx M_{char} \Omega \tau_{\star} \approx 300M_{\oplus}$ of characteristic-size particles is lost through blow out by radiation pressure. In order to replenish this loss, Wyatt *et al.* (2000) proposed that the IR-emitting μm -size particles are collisional fragments of larger parent particles. Unless we are observing HR 4796A in a special epoch, the total amount of mass in the parent particles (M_{tot}) is likely to be comparable to or larger than M_{lost}^{char} .

In the model presented by Telesco *et al.* (2000), only a single population of characteristic μm -size particles is assumed to be responsible for the reprocessing of stellar radiation. In order for the parent particles assumed by Wyatt *et al.* (2000) to remain inconspicuous, their total surface area must be less than that of the μm -size IR-emitting particles. For a population of parent particles to contribute a major fraction of M_{tot} , their total area is $\propto a_d^{-1}$. Since $M_{lost}^{char}/M_{char} \sim \Omega \tau_{\star} \sim 10^5$, the minimum size for the parent particles is $a_{min} \sim 10^5 a_c \sim 10\text{cm}$ such that their τ_z is less than that of the IR-emitting μm -size particles.

3.2. Particle collisions

The production of μm -size particles requires collisions. The collisional frequency for individual characteristic particles is

$$\nu_c \sim n_d A_d \sigma_d, \quad (25)$$

where σ_d is the velocity dispersion of the particles. The spatial number density of those particles which contribute to most of the IR radiation is

$$n_d = \frac{M_{char}}{m_d 4\pi R d R H_d} \simeq \frac{4R}{3dR} \frac{L_{disk}}{L_{\star}} \frac{\rho_d a_d}{m_d H_d}. \quad (26)$$

For photons with wavelength smaller than the characteristic size of the particles, the particles’ opacity is determined by their geometric cross section A_d . The optical depth in the direction normal to the plane of the disk is $\tau_z \sim (M_{char}/m_d)(A_d/2\pi R d R) \sim L_{disk}/L_{\star}$. From Eqs. (23) and (25) we find the collisional frequency for IR emitting particles to be

$$\nu_c \sim \nu_{cI} = \frac{R}{dR} \frac{L_{disk}}{L_{\star}} \Omega \sim \tau_z \Omega \ll \tau_d^{-1}. \quad (27)$$

If the dominant contributors of the IR radiation are μm -size particles as postulated by Wyatt *et al.* (2000), they would be blown out on a dynamical time-scale because their $a_d < a_1$ (in a gas-free

environment) and $a_d < a_2$ (when the particles are embedded in a gaseous disk). Thus, after they are produced from the collisions of their parent particles, these particles would not have sufficient time to collide, fragment, or coagulate among themselves before they are ejected of the ring region. Furthermore, in order for the μm -size particles to remain as the dominant IR emitters, both τ_z and ν_c must decrease with particle size so that the particles with $1 - 2\mu m < a_d < a_1$ or a_2 would not dominate the radiation reprocessing. Since both a_1 and a_2 are considerably larger than a few μm , the hypothetical μm -size IR-emitting particles must be produced directly (rather than through a cascade process) during collisions between the smallest surviving particles (those with $a_d > a_1$ or $a_d > a_2$).

We now consider the collision frequency of the population of parent particles which are the main suppliers of the μm -size IR-emitting particles. In the minimum-size (with $a_d \sim a_{min} \sim 10$ cm) limit, the parent particles' ν_c is comparable to that of the IR-emitting particles, *i.e.* ν_{cI} in eq(27). On the dynamical time-scale during which the μm -size particles are blown away, a total fraction $\nu_{cI}\tau_d$ of the parent particle population would collide. In order for this limited number of events to directly replenish the mass loss due to the radiative blow-away of the IR-emitting particles, each collision must generate $N_f \sim (\tau_\star/\tau_d)^2 L_\star/L_{disk} \sim 10^{12}$ (μm -size) fragments. The parent bodies could have a size $a_d > a_{min}$, in which case, collisions would occur less frequently by a factor $\sim a_{min}/a_d$ provided they can lead to the production of $\sim (\tau_\star/\tau_d)^2 (a_d L_\star/a_{min} L_{disk})$ fragments. Note that particles with sizes $> (\tau_\star L_{disk}/\tau_d L_\star) a_{min}$ collide less than once during τ_\star . Nevertheless, at least in principle, collisions among a fraction of the large-particle population may replenish the μm -size IR-emitting particles.

The considerations presented in this subsection indicate that the μm -size particle scenario suggested by Telesco *et al.* (2000) and Wyatt *et al.* (2000) requires not only a population of parent bodies which are larger than a few cm but also a non continuous bimodal ($\sim 1\mu m$ and $> 10cm$) particle-size distribution. There is no simple physical mechanism to preferentially produce this type of particle distribution function.

3.3. Particle size distribution

In reality, collisions are more likely to produce fragments with a range of sizes. As noted above that all fragments with $a_d > a_1$ (in a gas-free environment) or $a_d > a_2$ (if the fragments are embedded in a residual gaseous disk) would survive the radiative blow out. During the life span of HR4796A, the minimum-size parent particles would undergo $\nu_{cI}\tau_\star \sim (L_{disk}/L_\star)(\tau_\star/\tau_d) \sim 10^3$ collisions. Although fragmentary particles with $a_1 < a_d < a_{min}$ or $a_2 < a_d < a_{min}$ may collide less frequently, they may nevertheless attain a collisional coagulation-fragmentation equilibrium.

In principle, the particles' size distribution may be obtained by solving the appropriate coagulation equation with both coagulation and fragmentation effects included. Approximate solutions may be obtained for collisional steady state in which the disruption or growth rates (\dot{M}_d)

of the total mass ($M_d = N_d m_d$) for a given population may be assumed to be independent of a_d . If we assume the size-distribution evolution occurs primarily through collisions between similar size particles,

$$\dot{M}_d \simeq M_d \nu_c \sim N_d^2 m_d (a_d/R)^2 \Omega. \quad (28)$$

A constant \dot{M}_d would imply $N_d \propto a_d^{-2.5}$, $M_d \propto a_d^{0.5}$ and $\tau_z \propto a_d^{-0.5}$, *i.e.* most of the mass are contained in the large particles whereas most of the surface area cross sections are contained in the small particles. This particle size distribution is similar to that derived for collisional equilibrium (Hellyer 1970, Mathis *et al.* 1977) and adopted by Augereau *et al.* (1999) in which

$$dN_d/da_d \propto a_d^{-3.5}. \quad (29)$$

More generally, the growth and fragmentation may be mainly regulated by collisions between different-size particles, which would result in a slightly modified size distribution.

The distribution function in eq(29) is only applicable for particles with $a_d \sim a_1$ or $a_d \sim a_2$. Since smaller particles are subject to radiative blow out of the ring before they can collide with each other again, their size distribution is probably determined by that resulting from the break up of the parent bodies. But if this distribution function can be extended to the small particles the total mass carried by the blown-away dust particles is $M_{lost}^{tot} \sim M_{lost}^{char} (a_1/a_c)^{1/2} \simeq 5 - 10 \times 10^2 M_\oplus$ in the gas free environment and $M_{lost}^{tot} \sim M_{lost}^{char} (a_2/a_c)^{1/2} \simeq 3 \times 10^3 M_\oplus$ if the particles are embedded in a protostellar disk of gas. Note that the inferred values of M_{lost}^{char} and M_{lost}^{tot} are comparable to Jupiter and Saturn’s masses and the Oort’s cloud (Duncan, Quinn, & Tremaine 1987). This mass is larger than the present mass estimate ($\sim 0.1 M_\oplus$) for the Kuiper Belt today (Luu *et al.* 1997) but may be comparable to it in the past (Stern *et al.* 1997, Kenyon & Luu 1999). The associated surface density of heavy elements is also comparable to that extrapolated from the minimum mass nebula for $R_0 = 70\text{AU}$.

3.4. Preserved particle scenario

We now consider the possibility that a range of particles were formed inside a gaseous protostellar disk. When the surface density of the disk is depleted, particles in the outer regions of the disk become exposed to the stellar radiation, all particles with $a_d < a_2$ would be blown away by the radiation pressure. If these small particles are not the dominant IR emitters, they would not need to be continually replenished by some parent particle. In their model analyses of a large wavelength range of IR emission, Augereau *et al.* (1999) adopt a distribution of particles with sufficiently large size to survive radiation blow outs. We follow their approach by examining the evolution of the surviving particles.

Using our model parameters, we find $a_2 = 100 - 200 \mu m$ (see Fig. 1 and Fig. 2). (Note that a_2 does not directly depend on the gas surface density as long as $a_0 > a_2$). For illustrative simplicity, we assume the IR-emitting particles have a characteristic size $a_d = a_0 = 600 \mu m$ such that eq(24)

gives $M_{char} \sim 2.3M_{\oplus}$. Since these particles survive the radiation blow out, they collide up to $\sim \nu_c \tau_{\star} \sim (L_{disk}/L_{\star})(\tau_{\star}/\tau_d) \sim 10^3$ times within the life span of the central star.

In order to determine the collisional velocity among the particles, we note that in the absence of any warp, the optical depth in the disk’s radial direction to the host star is $\tau_r \sim \tau_z R/H_d$. Since the surface brightness of the disk is spread out over an extended radial range, $\tau_r < 1$ and $H_d/R > L_{disk}/L_{\star}$ for the IR emitting particles. The corresponding velocity dispersion of the particles would be $\sigma_d \geq 3 \times 10^3 \text{cm s}^{-1}$. If these particles are embedded in a gaseous background, H_d is expected to be $\leq H_p$ which corresponds to an upper limit $\sigma_d \leq 10^5 \text{cm s}^{-1}$. Within this velocity range, collisions may lead to either erosion (Hatzes *et al.* 1991) or coagulation if the particles are coated with frosts or traces of methanol as in comets Supulver (*et al.* 1997). Repeated collisions may eventually lead to an equilibrium in which fragmentation and coagulation are balanced to result in a size distribution similar to that in eq(29) (see review by Artymowicz 1997).

In addition to the mass requirement, a population of surviving particles (with $a_d > a_1$ and $a_d > a_2$) need to have a spatial distribution similar to that observed ring structure whether they are parent particles or the dominant IR emitting particles. In the following subsection we show that particles which are marginally larger than a_2 can conglomerate into rings if there are some non monotonic variations in the Σ distribution of the gas. However, if particles become larger than a_0 , they decouple from the gas flow. Nevertheless, this confinement mechanism continues to be effective provided dV become positive although the rate of concentration decreases with the particle size. Meter sized particles need $\approx 10^3$ times longer to concentrate as they radially drift about 10^3 times slower than the 600μ particles.

3.5. A set of quasi-static models

3.5.1. Model: A

We first consider the hydrostatic structure of both gas and dust disk. We set the initial surface density distribution of the gas to be proportional to $R^{-5/2}$ as it is typical for protostellar disks. The presence of gas is invoked in order to establish a flow with velocity reversal which would spontaneously lead to the emergence of ring structure. In §2.1, we adopt the surface density distribution of the gas disk to be that in eq (1) with its mass within 70 ± 20 AU to be $99M_{\oplus}$ in order to augment for the solar composition. As a free parameter, we set $d = 0.9$ which corresponds to a smooth 10% surface density increase at 70 AU. The amplitude of this variation in Σ (see Fig. 1 and Fig. 2) is much smaller than that associated with gap formation.

The disk structural parameters are calculated self-consistently for a dynamically stable, rotating, optical-thin disk. This equilibrium configuration is established on the dynamical time-scale τ_d . The increase in surface density of the gas at 70 AU corresponds to a minor peak in density, a local minimum in the friction time and stokes number, but it has no effect on

temperature and pressure scale height, because the disk is optical thin (Fig. 1). The pressure as function of density also shows a small amplitude local maximum. The resultant local maximum in the radial pressure gradient strongly influences the local rotational profile such that the deviation from the Keplerian rotation speed is decreased by 50%. The velocity resulting from the Poynting Robertson effect is orders of magnitude smaller and it attains this local minimum as a consequence of the decrease in the friction time τ_f (see eq. 5). The last frame shows the minimum radius for particles to be gravitationally bound (a_2), which is given in eq(18) by the equilibrium of the radiation pressure, gravity and centrifugal forces. This plot also indicates the upper particle size limit for particles to be stopped at 70AU, which is about $700 - 800\mu$.

For these disk parameters, our chosen particle's size is ($a_d = a_0 = 600\mu m$) to receive maximal velocities and thus to show the upper limit of concentration. In Fig. 3, the solid line represents the resulting drift velocity of these particles due to combined effect of gas drag and radiation pressure in accordance to eq(15). In order to consider the relative importance of various contributions, we compare our main results with the dashed-line velocity curve for particles in a gravity- and rotation-free system, where radial radiation pressure and friction forces cancel each other. In this idealized case, the particles' radial velocity is positive everywhere because the friction time grows faster than the radiation pressure decreases with radius. The decline in v_r at 70 AU is due to the local minimum in the friction time-scale.

We also show with the dotted line, the v_r distribution in a system where the radiation pressure is neglected and the orbital evolution is determined by gas drag only. In this limit, the radial drift is proportional to the friction time and the particles migrate inward everywhere. Due to the non monotonic variation in our prescribed Σ distribution near 70 AU, the deviation of the gas velocity from the Keplerian flow is at a minimum. This change in dV leads to a large increase in v_r . But with $d = 0.9$ and $\delta R_0 = 20AU$ in Model A, gas drag alone is not sufficient to change the sign of dV and v_r . In contrast, when the effects of radiation pressure and gas drag are fully taken into account simultaneously, a radial velocity inversion is established near 70 AU.

For this model, particles with $a_d < a_2$ are blown away by the radiation pressure on the dynamical time-scale τ_d . When the surface density of the gas is reduced below $\Sigma_2 \equiv 3L_\star / (8\pi R c c_s^3 \partial \ln \rho / \partial \ln R) \sim 0.1 \text{g cm}^{-2}$, a_0 becomes smaller than a_2 (see eq. 6 and eq. 18) and there are no longer particles that drift radially outward as a result of the combined forces from gas and radiation. If the motion of the disk gas is only affected by a negative pressure gradient, all particles with $a_d < a_0$ would be blown away by the stellar radiation pressure and all particles with $a_d > a_0$ would become segregated from the motion of the gas, drift inwards with a radial velocity in accordance to eq(17) and a corresponding orbital evolution time-scale $R/v_r \sim (R/H_p)^2 (a_d \rho_d / \Sigma) \tau_d \sim (R/H_p)^2 \tau_d$. In this case, all particles with sizes smaller than $\sim a_2 (H_p/R)^2 (\tau_\star / \tau_d)$ would be depleted during the lifespan of HR4796A. But Σ_2 is only marginally larger than the surface density of the parent particles inferred in §3.1. In §2.4, we have already shown that the particles' drag have a negligible effect on the motion of the gas. Eventually, when the surface density of the gas is reduce below $\Sigma_1 \equiv 3L_\star / (8\pi G M_\star c) \sim 10^{-2} \text{g cm}^{-2}$, $a_0 < a_1$. All

particles with $a_d < a_1$ are blown away by the radiation pressure whereas larger particles would not undergo further orbital decay as the effect of head wind diminishes.

3.5.2. Model: B

We also computed a model with the same d but a smaller $\delta R_0 = 10AU$ which represents a gaseous ring with a 2 times steeper surface density gradient (see Figs. 2 and 4). In this case, the gas rotation is hyper Keplerian with a sign change in dV such that gas drag alone may lead to an outward velocity near 70 AU. All particles with $a_d > a_2$ or $a_d > a_0$ would migrate outwards in regions with a positive pressure gradient and inwards in regions with a negative pressure gradient. In this case there is no upper limit for the particle size in order to be stopped at 70 AU. Fig. 5 shows that the resulting drift velocities for 1m sized objects is about three orders of magnitude smaller which nevertheless allows these bodies to concentrate in reasonable time in a ring at 70 AU.

3.6. Dynamical evolution

The resulting radial drift velocity (Eq. 15) can be used with the continuity equation to compute the global evolution of the dust surface density Σ_d as a result of their orbital migration. In a cylindrical coordinate system,

$$\frac{\partial \Sigma_d}{\partial t} = -\frac{1}{R} \frac{\partial}{\partial r} (R j_\Sigma). \quad (30)$$

The local flux of dust particles is partially contributed by the systematic radial drift v_r (see Eq. 15). Small particles with $a_d < a_0$, are well coupled to the disk gas. If the disk gas is turbulent, as in accretion disks in many astrophysical contexts (cf. Lin & Papaloizou 1996), these particles may undergo diffusion following the trace of turbulent eddies. For computational convenience, we describe the turbulent stirring as passive diffusion in the conventional Navier-Stokes equation such that

$$j_\Sigma = \Sigma_d v_r - \frac{D}{R} \frac{\partial}{\partial r} (R \Sigma_d). \quad (31)$$

A similar approach was used by Morfill and Völk (1984) to study the reprocessing of meteorites in the solar nebula. Following Cuzzi *et al.* (1993), we assume the turbulent diffusivity $D = \nu / Sc$ with the Schmitt number which describes the coupling between the particle and the gas is set to be $Sc = (1 + St)^{1/2}$. For the gas turbulent viscosity, we adopt the *ad hoc* α prescription which is commonly used in accretion disks (Shakura & Sunyaev 1973) such that

$$\nu = \alpha c_s H_p. \quad (32)$$

The Stokes number for particles is modified from that for a laminar disk (see §2.2.1) by

$$St = \tau_f \omega_t. \quad (33)$$

ω_t is the circular frequency of the largest eddy (typically smaller than Ω). Thus, from the definition of the effective viscosity it follows:

$$\omega_t = \frac{\nu}{H_p^2}. \quad (34)$$

For the particle size we are considering, the turbulent Schmitt number is ~ 1 so that maximum mixing is expected to occur.

The differential equation (30) is solved numerically using a finite volume scheme. It is integrated explicitly in time with a simple Euler backward scheme.

3.6.1. Model: A

In Figure 6 the initial radial Σ_d distribution of $600\mu m$ dust particles ($= 10^{-2}\Sigma$) is shown with the solid line. The evolution of the Σ_d distribution is shown with a series of dotted lines which represents time sequences separated by 10^3 yr between each line. After the first 400 yr, the dust particles inside 66AU drift inward while that between 66 and 69 AU drift outward. The lack of replenishment causes Σ_d interior to 66AU to decline. The results in Figure 3 indicate that v_r is a decreasing function of R (i.e. the magnitude of v_r is more negative at large R) inside 66 AU. Consequently, the depletion of the disk is more rapid at larger R and Σ_d becomes a decreasing function of R in this region. The outward drift at 66-69AU and inward drift at radius larger than 69AU cause the accumulation of dust particles between 67-73 AU and the depletion of dust exterior to 73 AU. After several 10^3 yr, an equilibrium is reached in which the turbulent diffusion is balanced by the systematic drifts. In this equilibrium, $\Sigma_d R$ between 67-73 AU becomes nearly two orders of magnitude larger than that of the disk interior to 67 AU and another two orders of magnitude larger than that of the disk beyond 73 AU. The actual width of the ring depends on the magnitude of the effective viscosity parameter. A much wider ring may be obtained for a larger viscosity $\alpha > 10^{-4}$.

After the equilibrium is established, the persistence of the gas is not required. In §2.2.2, we show that as Σ decreases during the depletion of the disk, a_0 decreases and τ_f increase while dV is not significantly modified. While a_d is still small compared with a_0 , the factor $(L_\star A_d / 4\pi R^2 mc + 2\Omega dV)$ in eq(15) remains unchanged. Although the magnitude of v_r may increase due to the weakening hydrodynamic drag effect, the locations for velocity reversal remain unaltered. Thus, dust particle concentration in the ring is not affected by the depletion of Σ . Although dust particles would generally migrate inwards after a_0 decreases below their size a_d , the drag time-scale becomes so large that the radial locations of the particles are preserved. Thus, this scenario only needs the gas to be present for the initial few 10^4 yrs in order to produce the ring. Afterwards it can be evaporated or be viscously diffused, while the dust distribution remains intact.

3.6.2. Model: B

Similar model parameter are applied to a narrower ring (with $\delta R_0 = 10AU$). In this model, we examine the concentration of $1m$ -size large objects. Fig. 7 shows the same behavior like the smaller particles, but this time the process is about 1000 times slower. Nevertheless, the concentration process takes an order of magnitude less time than the life time of HR4796A.

3.6.3. Model: C and D

So far the upper limit for the observed gas around HR4796A is $1-7 M_{\oplus}$ (Greaves *et al.* 1999), which is 1-2 orders of magnitude less than we used for Model A and Model B. Now we present to models with only $10 M_{\oplus}$ of gas (see fig. 8) and $1 M_{\oplus}$ (see fig. 9). In comparison to the first models the densities are smaller, the Stokes numbers for 600μ particles are bigger and thus the resulting drift velocities become also smaller. There are no significant changes in the critical particle size a_2 .

Thus the dynamical evolution takes 5 times longer for Model C (see fig. 10) and about 25 times longer for Model D (see fig. 11). Even the time-scales increase at lower gas densities, the general effect persists.

4. Summary and Discussions

We examined in this paper the dynamics of the dust ring around HR 4796A with two separate scenarios. In the first scenario, we consider the case where the dominant emitters of the IR radiation are μm -size particles. Since these particles are being blown away by the radiation pressure of the central star, they must be replenished by large particles which are not affected by such a process. In a gas-free case, the parent particles must have a size greater than $\sim 3.2 \mu m$ whereas in a gas-rich environment, another order of magnitude larger size is needed. In order to account for the magnitude of reprocess radiation, $M_{char} \sim 4 - 8 \times 10^{-3} M_{\oplus}$ of μm -size particles are needed at any given time. During the life span of HR4796A, a total mass $M_{lost}^{char} \sim M_{char} \tau_{*} / \tau_d \sim 300 M_{\oplus}$ is needed in the reservoir of parent particles. In order for the parent particles to be inconspicuous sources of IR radiation relative to the μm -size particles, a large fraction of M_{lost} must be contained in particles with $a_d > 10cm$. However, the smallest surviving particles (with sizes $\sim 100 - 200 \mu m$), could provide adequate supplies of μm size particles if a large fraction of their mutual collisions results in their total fragmentation.

The main difficulty of identifying small particles as the dominant contributors of the IR radiation is the requirement of a non continuous bimodal size distribution. This problem would be removed if the particles which emit most of the IR radiation are sufficiently large ($> 100 \mu m$) to survive the radiative blow out. In this case, a total mass $< 0.4 M_{\oplus}$ is needed throughout the life span of HR 4796A. We suggest the preservation of these modest-size particles (whether they are

parent particles or the dominant IR emitters) is due to the combined effect of radiation pressure and gas drag.

We presented a detailed model for the formation of dust rings in circumstellar disks. Our model can account for rings with sharply defined edges if it is embedded in a gas disk. A very small amount of inhomogeneity is needed to induce the congregation of the particles. This inhomogeneity can be the result of a planet, but it does not necessarily has to be so. Photo-evaporation, an inhomogeneous initial distribution of mass after the infall, or inhomogeneities in the radial viscous transport of material can also account for such an anomaly in the surface density distribution. Thus we conclude that dust rings with sharp structures are not necessarily good indicator for embedded planets.

We thank D. Trilling and P. Bodenheimer for useful conversation. This work is supported in part through National Science Foundation grant AST-9618548, NASA grants NAG5-4277, 4494, 7515, and a special NASA astrophysics theory programme which supports a joint Center for Star Formation Studies at NASA-Ames Research Center, UC Berkeley, and UC Santa Cruz.

REFERENCES

- Artymowicz, P. 1997, *Annual Review of Earth and Planetary Sciences*, 25, 175
- Augereau, J.C., Lagrange, A.M., Mouillet, D., Papaloizou, J.C.B., & Gorod, P.A. 1999 *A&A*, 348, 557
- Backman, D.E., & Paresce, F. 1993, *Protostars and Planets III*, ed. E.H. Levy & J.I. Lunine (Tucson: Univ. of Arizona Press), 1253
- Beckwith, S.V.W., & Sargent, A.I. 1993a, in *Protostars and Planets III*, ed. E.H. Levy & J.I. Lunine (Tucson: Univ. of Arizona Press), 521
- Beckwith, S.V.W., & Sargent, A.I. 1993b, *ApJ*, 402, 280
- Beckwith, S.V.W., Sargent, A.I., Chini, R.S., & Güsten, R. 1990, *AJ*, 99, 924
- Bell, K.R., Cassen, P.M., Klahr, H.H., & Henning, Th. 1997, *ApJ*, 486, 372
- Boss, A.P. 1998, *ApJ*, 503, 923
- Burkert, A., & Bodenheimer, P. 1996, *MNRAS*, 280, 1190
- Cameron, A.G.W. 1978, *Moon and the Planets*, 18, 5
- Chiang, E.I., & Goldreich, P. 1997, *ApJ*, 460, 368
- Cuzzi, J.N., Dobrovolskis, A.R., & Champney, J.M. 1993, *Icarus*, 106, 102

- Cuzzi, J.N., Lissauer, J.J., Esposito, L.W., Holberg, J.B., Marouf, E.A., Tyler, G.L., & Boischot, A. 1984, in *Planetary Rings*, ed. R. Greenberg & A. Brahic (Tucson: Univ. of Arizona Press), 1984, 73
- Duncan, M., Quinn, T., & Tremaine, S. 1987, *AJ*, 94, 1330
- Elliott, J.L., & Nicholson, P.D. 1984, in *Planetary Rings*, ed. R. Greenberg & A. Brahic (Tucson: Univ. of Arizona Press), 1984, 25
- Goldreich, P., & Tremaine, S. 1978, *Icarus*, 34, 240
- Goldreich, P., & Tremaine, S. 1979, *Nature*, 277, 97
- Goldreich, P., & Tremaine, S. 1982, *ARA&A*, 20, 249
- Greaves, J.S., Mannings, V., & Holland, W.S. 2000 *Icarus*, 143, 155
- Grün, E., Zook, H.A., Fechtig, H., & Giese, R.H. 1985, *Icarus*, 62, 244
- Gustafson, B. 1994 *ARA&A*, 22, 553
- Hartmann, L., Calvet, N., Gullbring, E., & D'Alessio, P. 1998, *ApJ*, 495, 385
- Hatzes, A.P., Bridges, F., Lin, D.N.C., & Sachtjen, S. 1991, *Icarus*, 89, 113 Goldreich, P., & Tremaine, S. 1982, *ARA&A*, 20, 249
- Hayashi, C., Nakazawa, K., & Nakagawa, Y. 1985, *Protostars and Planets II*, ed. D.C. Black & M.S. Mathews (Tucson: Univ. of Arizona Press), 1100
- Hellyer, B. 1970, *MNRAS*, 148, 383
- Hillenbrand, L.A., Strom, S.E., Calvet, N., Merrill, K.M., Gatley, I., Makidon, R.B., Meyer, M.R., Skrutskie, M.F. 1998, *AJ*, 116, 1816
- Jayawardhana, R., Fisher, R.S., Hartmann, L.W., Telesco, C.M., Pina, R.K., & Fazio, G. 1998, *ApJ*, 503, L79
- Jensen, E.L.N., & Mathieu, R.D. 1997, *AJ*, 114, 301
- Jura, M., Zuckerman, B., Becklin, E.E., & Smith, R.C. 1993, *ApJ*, 418, L37
- Jura, M., Ghez, A.M., White, R.J., McCarthy, D.W., Smith, R.C., & Martin, P.G. 1995, *ApJ*, 445, 451
- Klahr, H.H., & Henning, Th. 1997, *Icarus*, 128, 213
- Koerner, D.W., Ressler, M.E., Werner, M.W., & Backman, D.E. 1998, *ApJ*, 503, 83

- Kenigl, A. & Ruden, S.P. 1993, *Protostars and Planets III*, ed. E.H. Levy & J.I. Lunine (Tucson: Univ. of Arizona Press), 641
- Kenyon, S.J., & Luu, J.X. 1999, *AJ*, 118, 1101
- Korycansky, D.G., & Papaloizou, J.C.B. 1995, *MNRAS*, 274, 85
- Lin, D.N.C., & Bodenheimer, P. 1981, *ApJ*, 246, 972
- Lin, D.N.C., & Papaloizou, J.C.B. 1979, *MNRAS*, 188, 191
- , 1985, *Protostars and Planets II*, ed. D.C. Black & M.S. Mathews (Tucson: Univ. of Arizona Press), 981
- , 1993, *Protostars and Planets III*, ed. E.H. Levy & J.I. Lunine (Tucson: Univ. of Arizona Press), 749
- Lin, D.N.C., & Papaloizou, J.C.B. 1996, *ARA&A*, 34, 703
- Lissauer, J.J. 1993, *ARA&A*, 31, 129
- Luu, J., Jewitt, D., Trujillo, C.A., Hergenrother, C.W., Chen, J., & Offutt, W.B. 1997, *Nature*, 387, 573
- Lynden-Bell, D., & Pringle, J.E. 1974, *MNRAS*, 168, 603
- Mathis, J.S. Rumpl, W., & Nordsieck, K.H. 1977, *ApJ*, 217, 425
- Morfill, G.E., & Völk, H.J. 1984, *ApJ*, 287, 371
- Mundy, L.G., Looney, L.W., Erickson, W., Grossman, A., Welch, W.J., Forster, J.R., Wright, M.C.H., Plambeck, R.L., Lugten, J., Thornton, D.D. 1996, *ApJ*, 464, 169
- Morfill, G.E., & Völk, H.J. 1984, *ApJ*, 287, 371
- Nakagawa, Y., Sekiya, M., & Hayashi, C. 1986, *Icarus*, 67, 375
- Nelson, A.F., Benz, W., Adams, F.C., Arnett, D. 1998, *ApJ*, 502, 342
- Pollack, J.B., Hubickyj, O., Bodenheimer, P., Lissauer, J.J., Podolak, M., & Greenzweig, Y. 1996, *Icarus*, 124, 62
- Preibisch, T., Sonnhalter C., & Yorke, H.W. 1995, *A&A*, 299, 144
- Ruden, S., & Lin, D.N.C. 1986, *ApJ*, 308, 883
- Ruden, S.P., & Pollack, J.B. 1991, *ApJ*, 375, 740
- Safronov, V.S. 1969, NASA TTF-677

- Schneider, G., Smith, A.S., Becklin, E.E., Koerner, D.W., Meier, R., Hines, D.C., Lowrance, P.J., Terrile, R.J., Thompson, R.I., & Rieke, M. 1999, *ApJ*, 513, 127
- Shakura, N.I., & Sunyaev, R.A. 1973, *A&A*, 24, 337
- Shu, F.H., Johnstone, D., & Hollenback, D. 1993, *Icarus*, 106, 92
- Shu, F.H., Najita, J., Ostriker, E., Wilkin, F., Ruden, S. & Lizano, S. 1994, *ApJ*, 429, 781
- Smith, B.A., & Terrile, R.J. 1984, *Science*, 226, 1421
- Stauffer, J.R., Hartmann, L.W., & Navascues, D.B. 1995, *ApJ*, 454, 910
- Stern, S.A., McKennon, W.B., & Lunine, J.I. 1997, in *Pluto and Charon*, 605
- Supulver, K.D., Bridges, F.G., Tiscareno, S., Lievore, J., Lin, D.N.C. 1997, *Icarus*, 129, 539
- Telesco, C.M., Fisher, R.S., Pina, R.K., Knacke, R.F., Dermott, S.F., Wyatt, M.C., Grogan, K., Holmes, E.K., Ghez, A.M., Prato, L., Hartmann, L.W., & Jayawardhana, R. 2000, *ApJ*, 528, in press
- Toomre, A. 1964, *ApJ*, 139, 1217
- Weidenschilling, S.J. 1977, *MNRAS*, 180, 57
- Weinberger, A.J., Becklin, E.E., Schneider, G., Smith, B.A., Lowrance, P.J., Silverstone, M.D., Zuckerman, B., & Terrile, R.J. 1999, *ApJ*, 525, 53
- Wetherill, G.W. 1980, *ARA&A*, 18, 77
- Whipple, F.L. 1972, in *From Plasma to Planet*, Proceedings of the Nobel Symposium 21, ed. A. Elvius (New York: Wiley), 211
- Wyatt, M.C., Dermott, S.F., Telesco, C.M., Fisher, R.S., Grogan, K., Holmes, E., & Pina, R.K. 2000, *ApJ*, in press
- Yorke, H., Bodenheimer, P., & Laughlin, G. 1995, *ApJ*, 443, 199
- Zuckerman, B., Forveille, T., & Kastner, J.H. 1995, *Nature*, 373, 494

Fig. 1.— Model A: The radial distribution of surface density, density, temperature, friction time for 600 μ -size particles, the resulting Stoke-Number, pressure scale height, the speed of sound, the pressure, the radial pressure gradient, the deviation from the Kepler rotational profile, the Poynting-Robertson effect and the size (cm) of the smallest gravitationally bound particles. The physical parameters for this plot are given by the mass ($M_\star = 2.5M_\odot$) and luminosity ($L_\star = 35L_\odot$) of the central object. Additional model parameters include the location of the maximum in surface density at $70AU$, the width of the inner edge as $\delta R_0 = 20AU$ and the gas mass around the edge between $R_0 - \delta R_0$ and $R_0 + \delta R_0$ which is taken to be 100 earth masses.

Fig. 2.— Model B: The radial distribution of surface density, density, temperature, friction time for 600 μ -size particles, the resulting Stoke-Number, pressure scale height, the speed of sound, the pressure, the radial pressure gradient, the deviation from the Kepler rotational profile, the Poynting-Robertson effect and the size of the smallest gravitationally bound particles. The physical parameters for this plot are given by the mass ($M_\star = 2.5M_\odot$) and luminosity ($L_\star = 35L_\odot$) of the central object. Additional model parameters include the location of the maximum in surface density at $70AU$, the width of the inner edge which is $\delta R_0 = 10AU$ and the gas mass around the edge between $R_0 - \delta R_0$ and $R_0 + \delta R_0$ which is 100 earth masses.

Fig. 3.— Radial velocities distribution of 600 μ -size particles for the model in Fig. 1. The solid line gives the effective radial drift. The dotted line accounts only for the gas-drag effect and the dashed line denotes only for the radiation pressure effect.

Fig. 4.— Radial velocity distribution of 600 μ -size particles for the model in Fig. 2. The solid line gives the effective radial drift.

Fig. 5.— Radial velocity distribution of 1 m -size particles for the model in Fig. 2. The solid line gives the effective radial drift.

Fig. 6.— Model A: Evolution of the 600 μ -size particle surface density distribution for the model in Fig. 1. The solid line gives the initial distribution. The following lines are snapshots every 400 yrs.

Fig. 7.— Model B: Evolution of the 1 m -size particle surface density distribution for the model in Fig. 2. The solid line gives the initial distribution. The following lines are snapshots every 10^5 yrs.

Fig. 8.— Model C: The radial distribution of surface density, density, temperature, friction time for 600 μ -size particles, the resulting Stoke-Number, pressure scale height, the speed of sound, the pressure, the radial pressure gradient, the deviation from the Kepler rotational profile, the Poynting-Robertson effect and the size of the smallest gravitationally bound particles. The physical parameters for this plot are given by the mass ($M_\star = 2.5M_\odot$) and luminosity ($L_\star = 35L_\odot$) of the central object. Additional model parameters include the location of the maximum in surface density at $70AU$, the width of the inner edge which is $\delta R_0 = 10AU$ and the gas mass around the edge between $R_0 - \delta R_0$ and $R_0 + \delta R_0$ which is 10 earth masses.

Fig. 9.— Model D: The radial distribution for surface density, density, temperature, friction time for 600 μ -size particles, the resulting Stoke-Number, pressure scale height, the speed of sound, the pressure, the radial pressure gradient, the deviation from the Kepler rotational profile, the Poynting-Robertson effect and the size of the smallest gravitationally bound particles. The physical parameters for this plot are given by the mass ($M_\star = 2.5M_\odot$) and luminosity ($L_\star = 35L_\odot$) of the central object. Additional model parameters include the location of the maximum in surface density at $70AU$, the width of the inner edge which is $\delta R_0 = 10AU$ and the gas mass around the edge between $R_0 - \delta R_0$ and $R_0 + \delta R_0$ which is 1 earth mass.

Fig. 10.— Model C: Evolution of the 600 μ -size particle surface density distribution for the model in Fig. 8. The solid line gives the initial distribution. Other lines are separated by a time interval of 2000 yrs.

Fig. 11.— Model D: Evolution of the 600 μ -particle surface density distribution for the model in Fig. 9. The solid line gives the initial distribution. The other lines are separated by time intervals of every 10^4 yrs.

Fig. 1

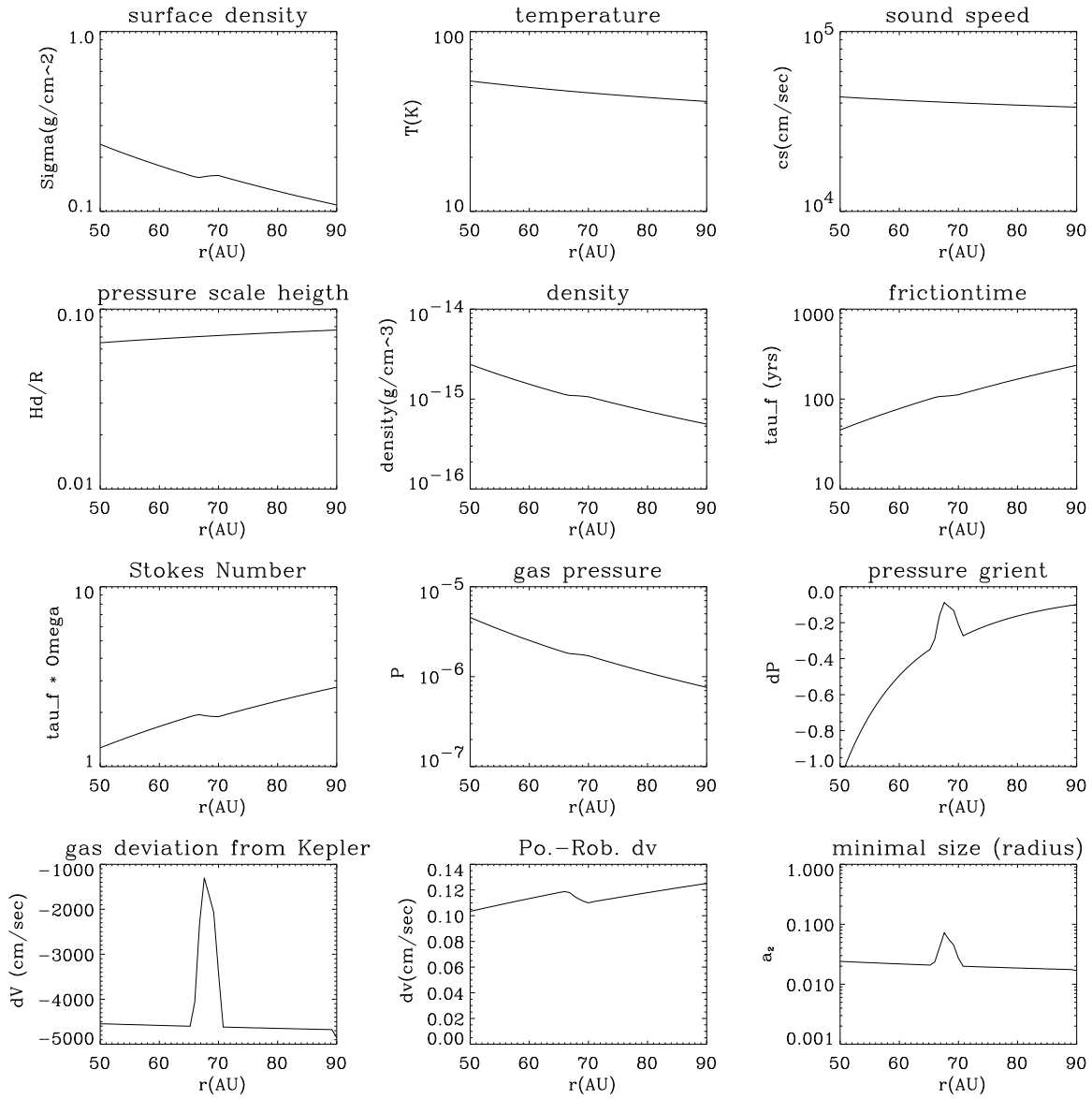


Fig. 2

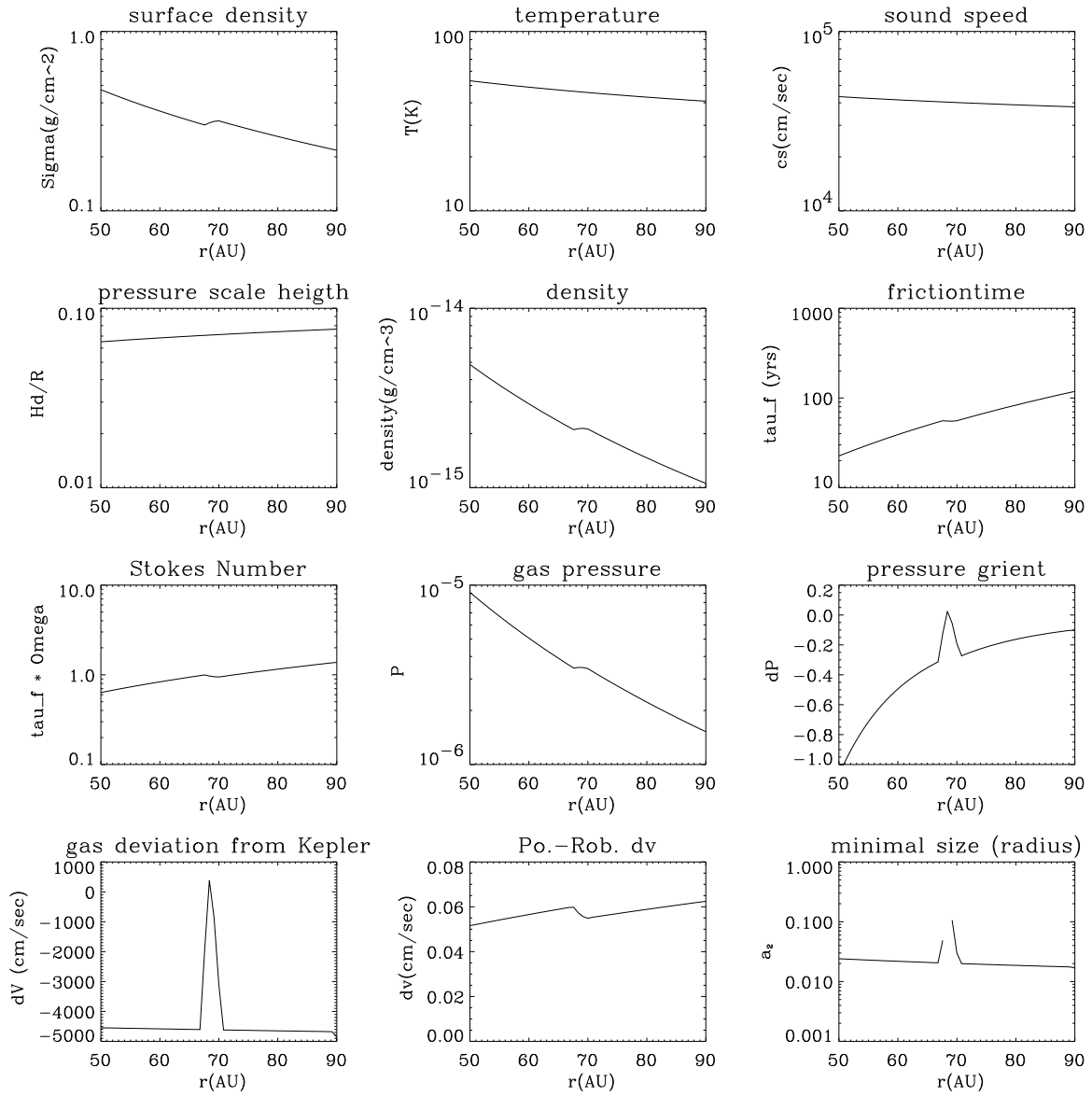


Fig. 3

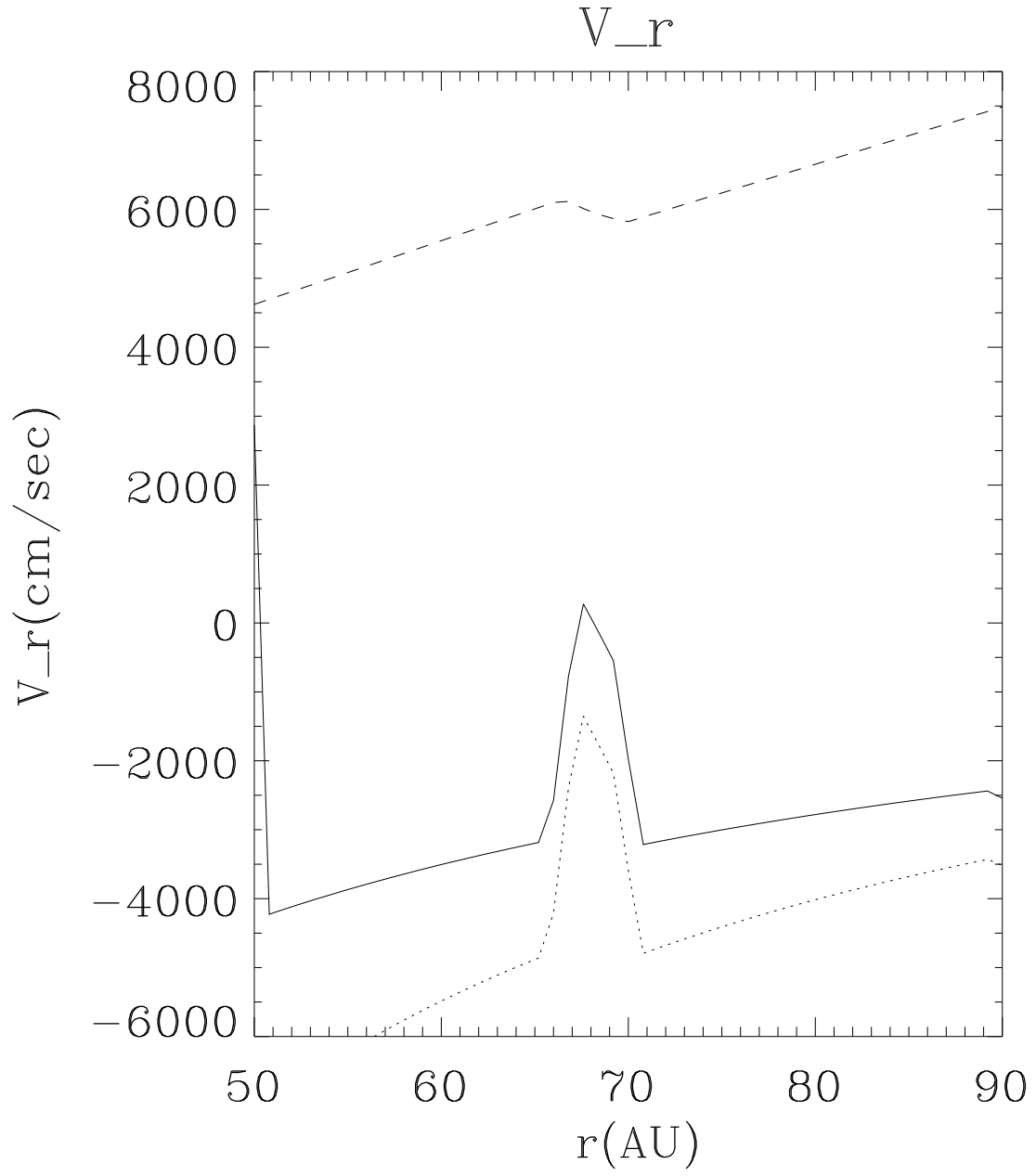


Fig. 4

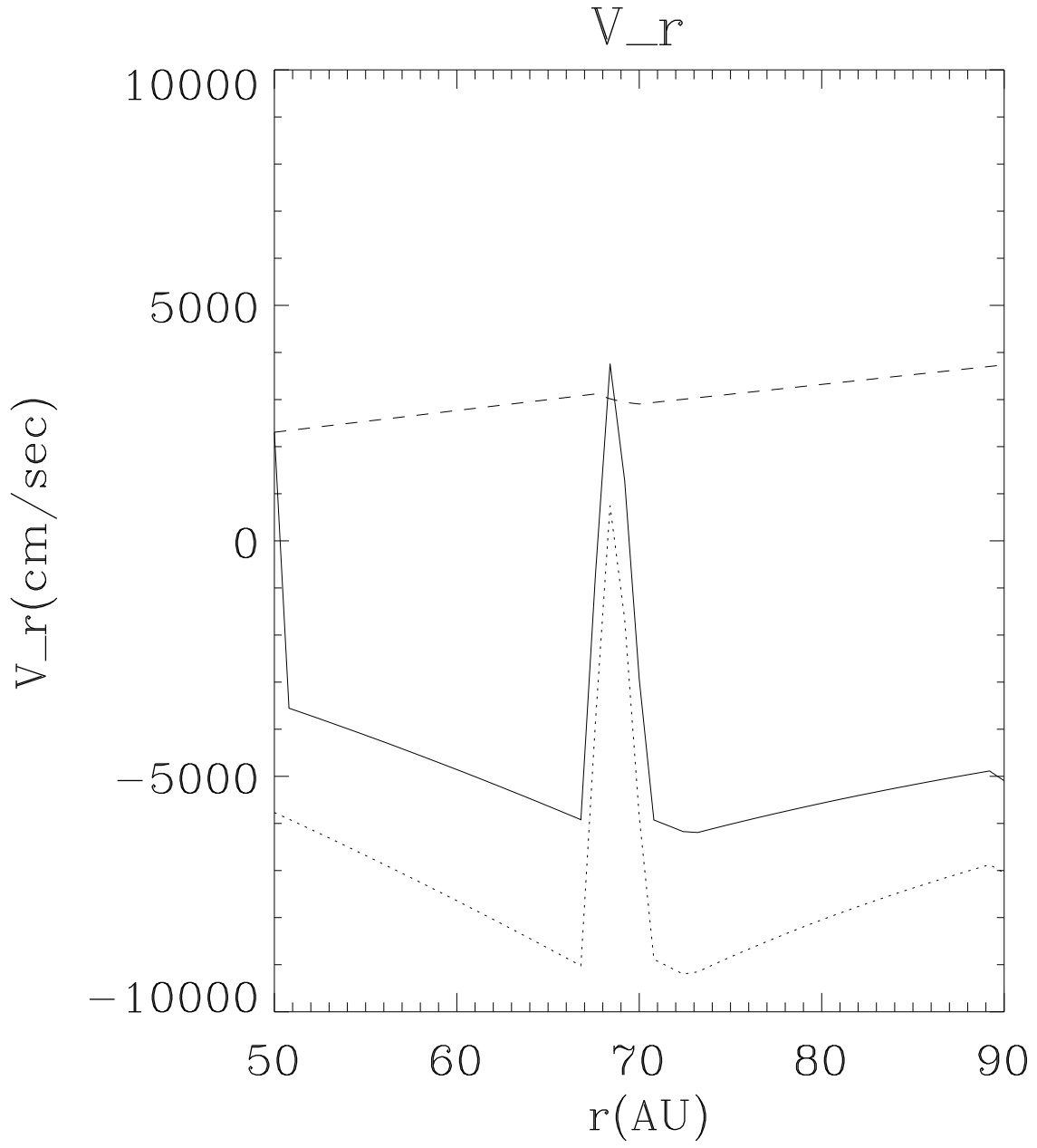


Fig. 5

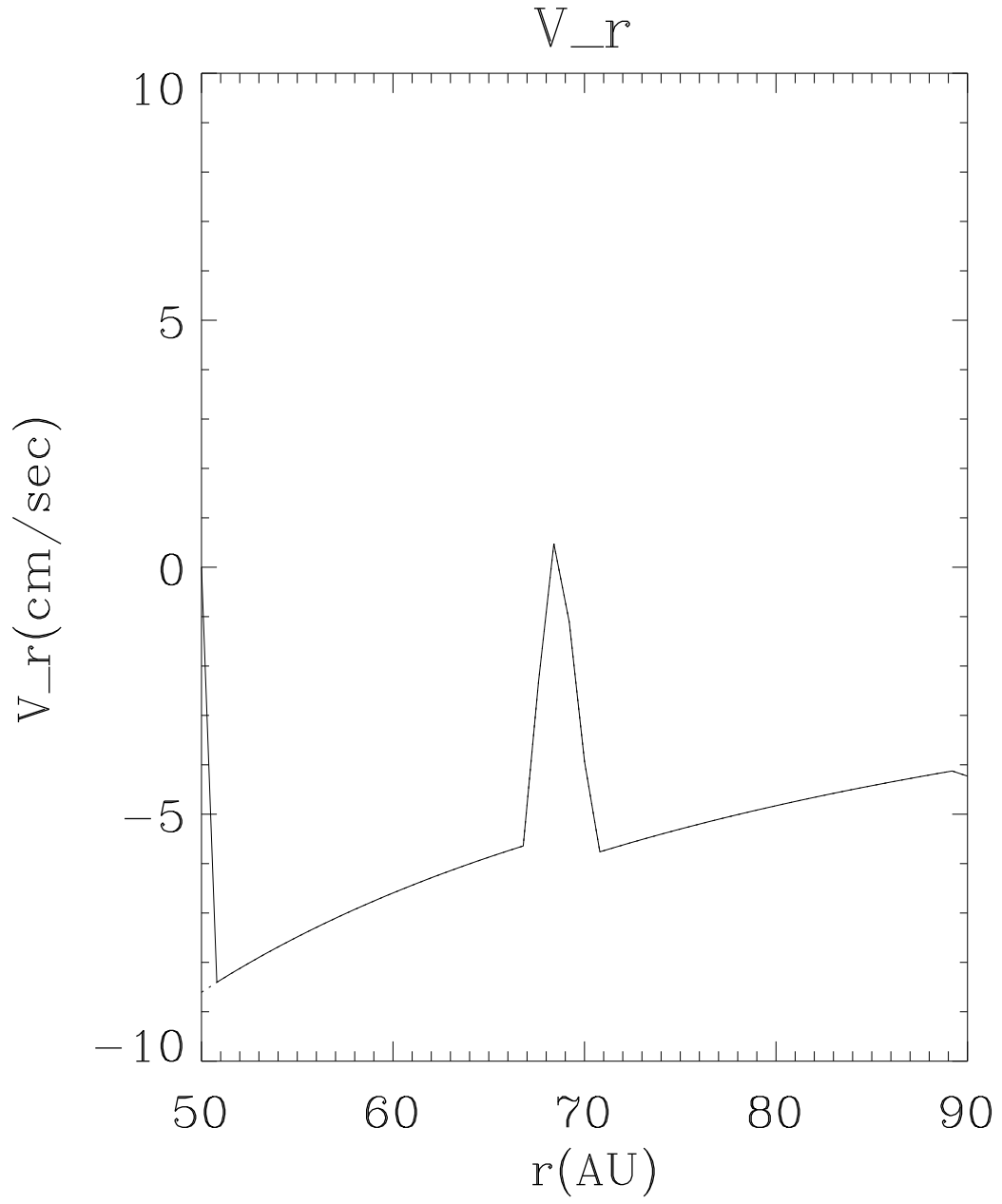


Fig. 6

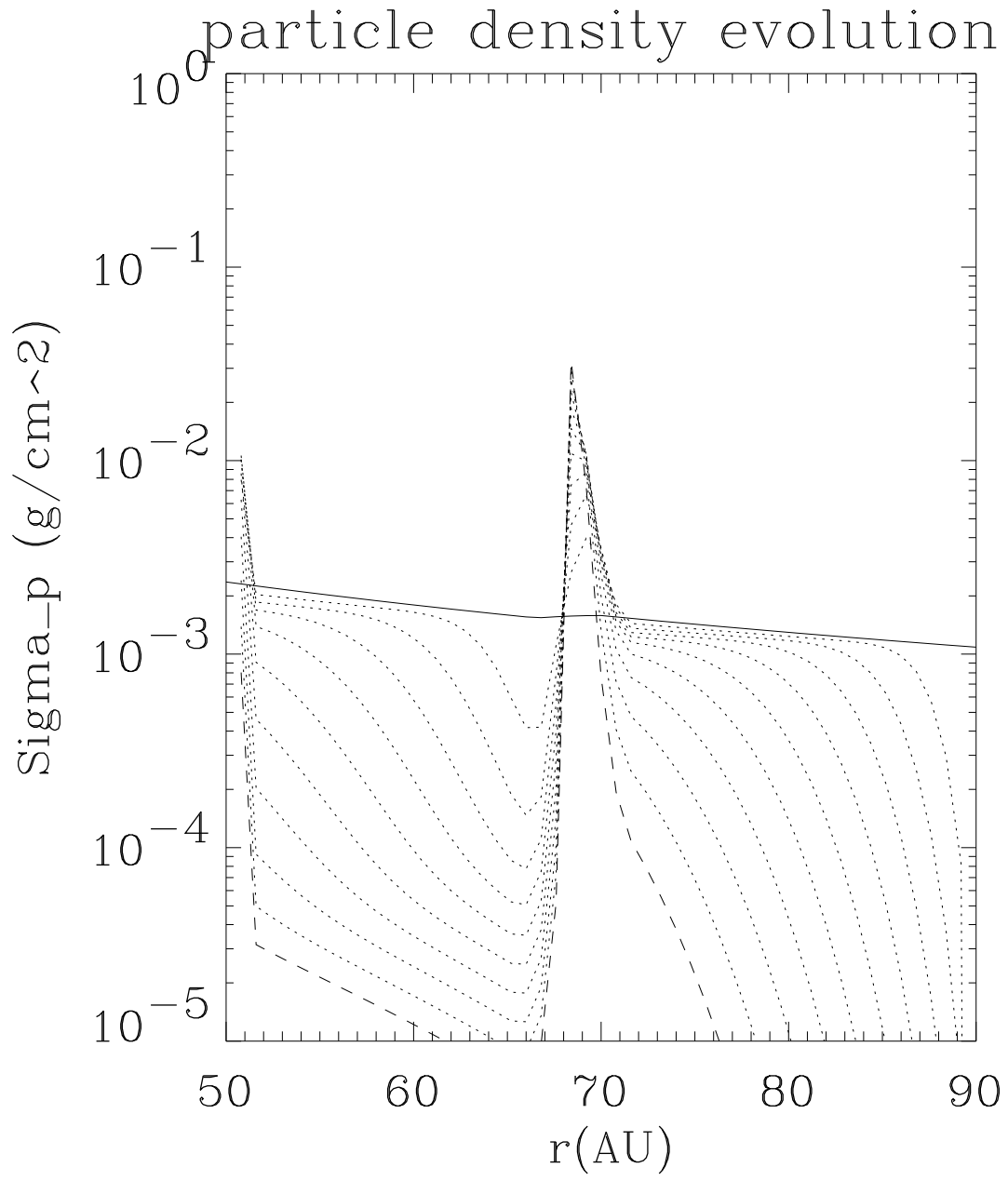


Fig. 7

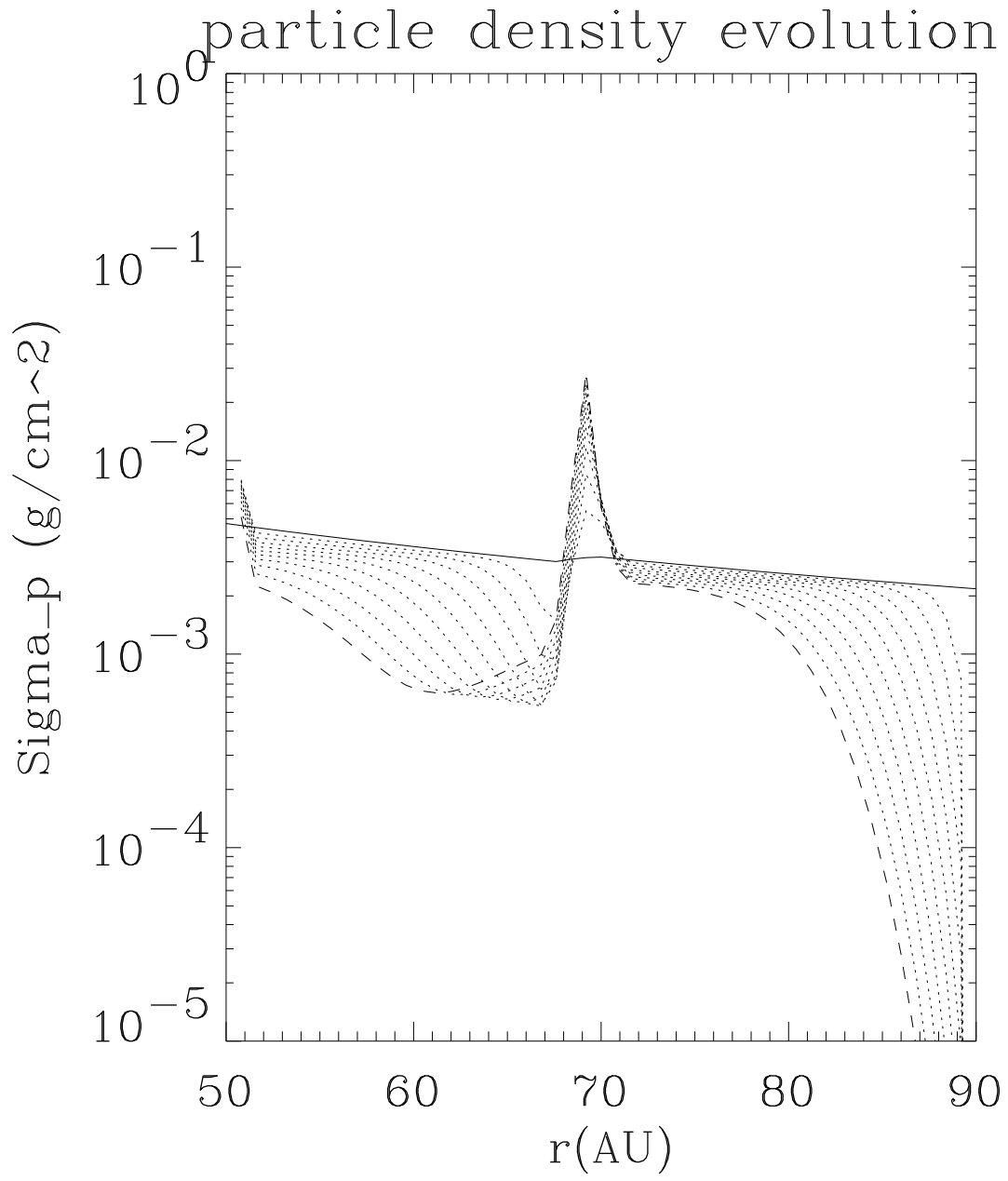


Fig. 8

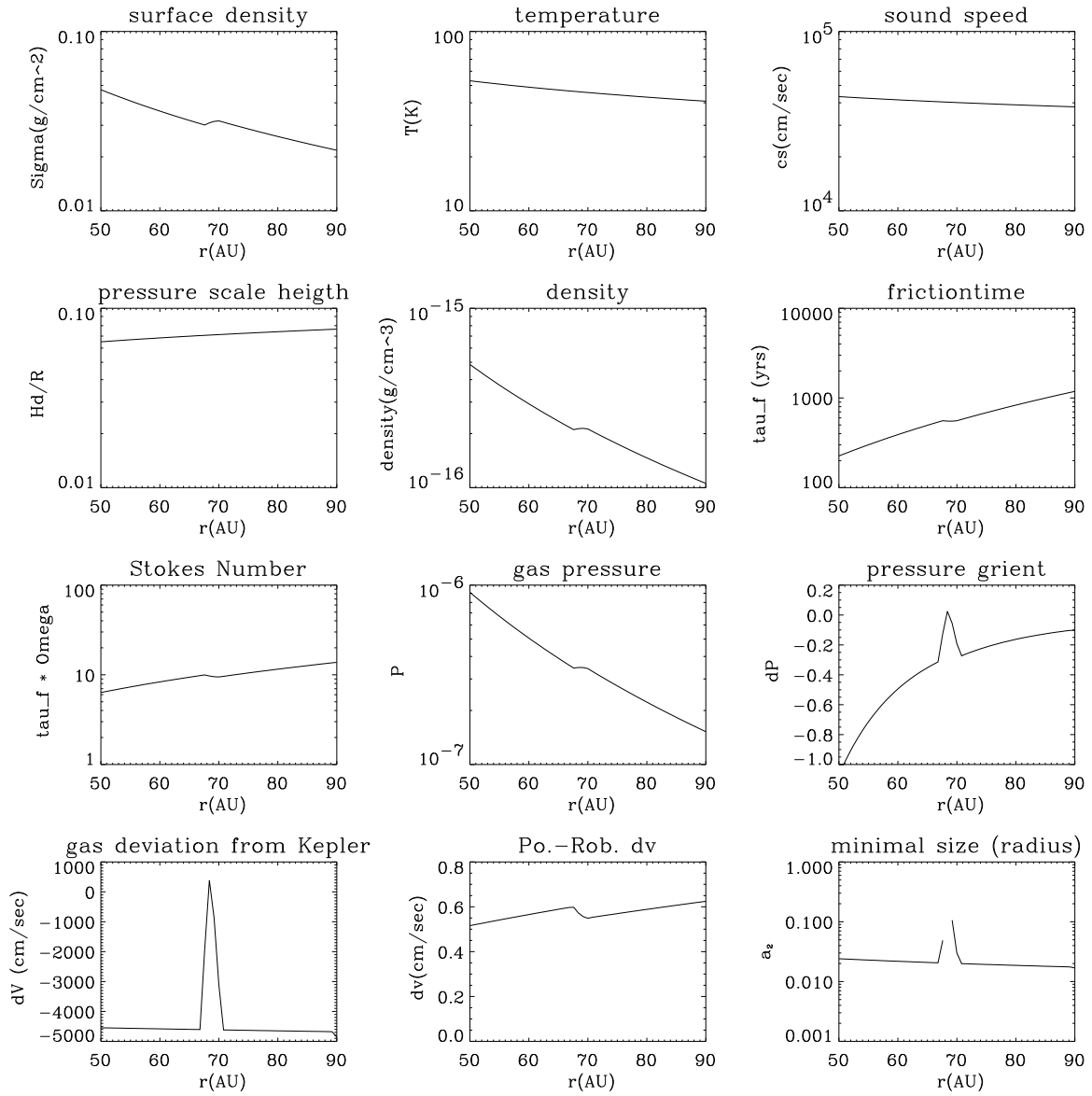


Fig. 9

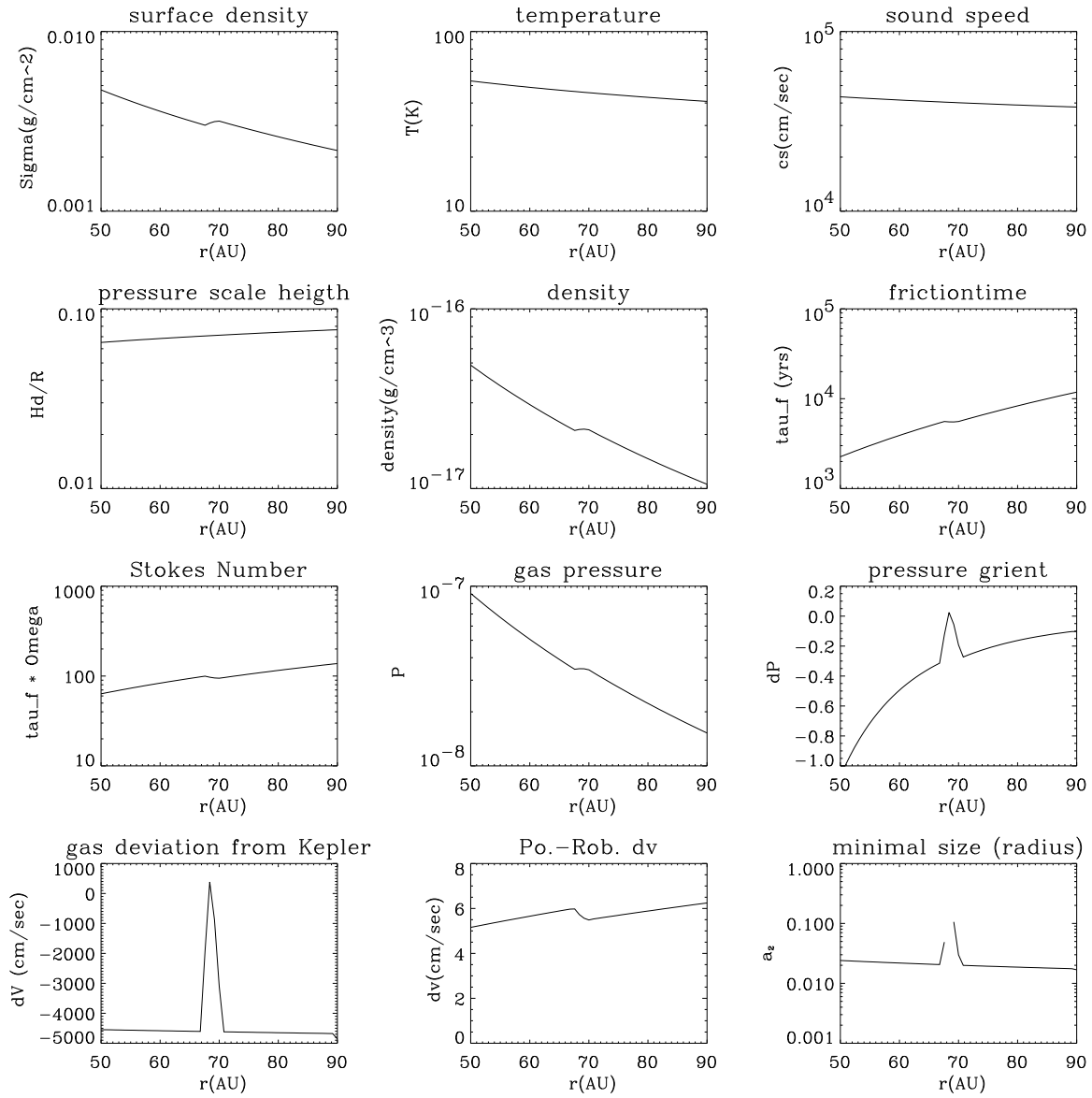


Fig. 10

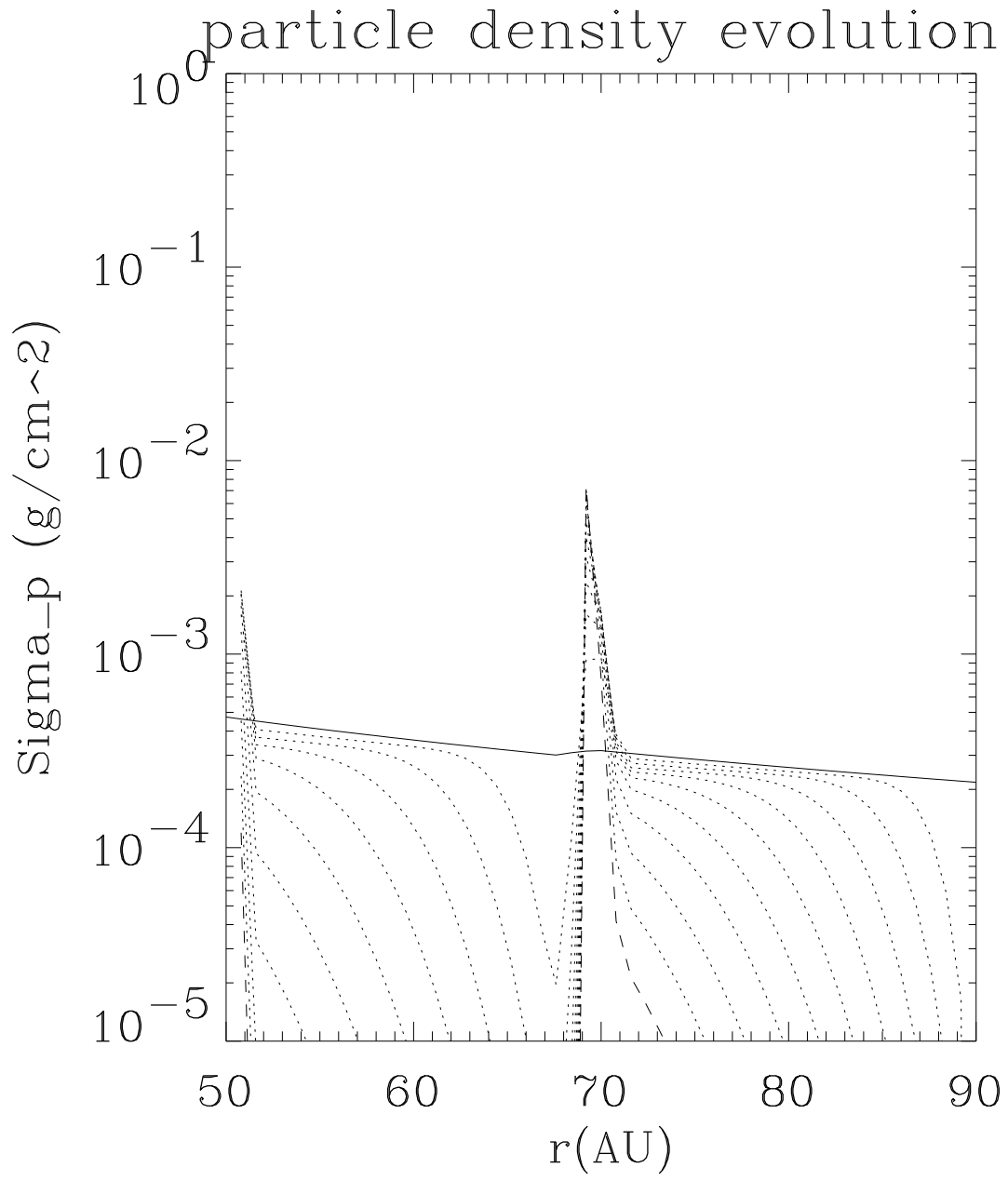


Fig. 11

